activation of the innate immune system. Our results may have important implications for the development of a safe and efficient *in vivo* siRNA delivery system that mediates RNAi but with minimal induction of immune activation.

## Acknowledgements

We thank Dr. G.L. Scherphof for his helpful advice in writing the English manuscript. This work was supported in part by Health and Labour Sciences Research Grants for Research on Advanced Medical Technology from the Ministry of Health, Labour and Welfare of Japan.

## References

[1] S. Akhtar, I.F. Benter, Nonviral delivery of synthetic siRNAs in vivo, J. Clin. Invest. 117 (2007) 3623–3632.
[2] M.A. Behlke, Progress towards in vivo use of siRNAs, Mol. Ther. 13 (2006) 644–670.
[3] P. Kumar, H. Wu, J.L. McBride, K.E. Jung, M.H. Kim, B.L. Davidson, S.K. Lee, P. Shankar, N. Manjunath, Transvascular delivery of small interfering RNA to the central nervous system, Nature 448 (2007) 39–43.
[4] Y. Sato, K. Murase, J. Kato, M. Kobune, T. Sato, Y. Kawano, R. Takimoto, K. Takada, K. Miyanishi, T. Matsunaga, T. Takayama, Y. Niitsu, Resolution of liver cirrhosis using vitamin A-coupled liposomes to deliver siRNA against a collagen-specific chaperone, Nat. Biotechnol. 26 (2008) 431–442.
[5] P.L. Felgner, T.R. Gadek, M. Holm, R. Roman, H.W. Chan, M. Wenz, J.P. Northrop, G.M. Ringold, M. Danielsen, Lipofection: a highly efficient, lipid-mediated DNA-transfection procedure, Proc. Natl Acad. Sci. USA 84 (1987) 7413–7417.
[6] Y.C. Tseng, S. Mozumdar, L. Huang, Lipid-based systemic delivery of siRNA, Adv. Drug Deliv. Rev. 61 (2009) 721–731.
[7] A.D. Judge, M. Robbins, I. Tavakoli, J. Levi, L. Hu, A. Fronda, E. Ambegia, K. McClintock, I. MacLachlan, Confirming the RNAi-mediated mechanism of action of siRNA-based cancer therapeutics in mice, J. Clin. Invest. 119 (2009) 661–673.
[8] N. Yagi, I. Manabe, T. Tottori, A. Ishihara, F. Ogata, J.H. Kim, S. Nishimura, K. Fujiu, Y. Oishi, K. Itaka, Y. Kato, M. Yamauchi, R. Nagai, A nanoparticle system specifically designed to deliver short interfering RNA inhibits tumor growth in vivo, Cancer Res. 69 (2009) 6531–6538.
[9] D. Papahadjopoulos, T.M. Allen, A. Gabizon, E. Mayhew, K. Matthay, S.K. Huang, K.D. Lee, M.C. Woodle, D.D. Lasic, C. Redemann, Sterically stabilized liposomes: improvements in pharmacokinetics and antitumor therapeutic efficacy, Proc. Natl Acad. Sci. USA 88 (1991) 11460–11464.
[10] W. Li, F.C. Szoka Jr., Lipid-based nanoparticles for nucleic acid delivery, Pharm. Res. 24 (2007) 438–449.
[11] Y. Matsumura, H. Maeda, A new concept for macromolecular therapeutics in cancer chemotherapy: mechanism of tumoritropic accumulation of proteins and the antitumor agent smancs, Cancer Res. 46 (1986) 6387–6392.
[12] E.T. Dams, P. Laverman, W.J. Oyen, G. Storm, G.L. Scherphof, J.W. van Der Meer, F.H. Corstens, O.C. Boerman, Accelerated blood clearance and altered biodistribution of repeated injections of sterically stabilized liposomes, J. Pharmacol. Exp. Ther. 292 (2000) 1071–1079.
[13] T. Ishida, H. Kiwada, Accelerated blood clearance (ABC) phenomenon upon repeated injection of PEGylated liposomes, Int. J. Pharm. 354 (2008) 56–62.
[14] T. Ishida, R. Maeda, M. Ichihara, K. Irimura, H. Kiwada, Accelerated clearance of PEGylated liposomes in rats after repeated injections, J. Control. Release 88 (2003) 35–42.
[15] T. Ishida, M. Ichihara, X. Wang, H. Kiwada, Spleen plays an important role in the induction of accelerated blood clearance of PEGylated liposomes, J. Control. Release 115 (2006) 243–250.
[16] T. Ishida, M. Ichihara, X. Wang, K. Yamamoto, J. Kimura, E. Majima, H. Kiwada, Injection of PEGylated liposomes in rats elicits PEG-specific IgM, which is responsible for rapid elimination of a second dose of PEGylated liposomes, J. Control. Release 112 (2006) 15–25.
[17] T. Tagami, K. Nakamura, T. Shimizu, T. Ishida, H. Kiwada, Effect of siRNA in PEG-coated siRNA-lipoplex on anti-PEG IgM production, J. Control. Release 137 (2009) 234–240.
[18] V. Hornung, M. Guenthner-Biller, C. Bourquin, A. Ablasser, M. Schlee, S. Uematsu, A. Noronha, M. Manoharan, S. Akira, A. de Fougerolles, S. Endres, G. Hartmann, Sequence-specific potent induction of IFN-alpha by short interfering RNA in plasmacytoid dendritic cells through TLR7, Nat. Med. 11 (2005) 263–270.
[19] M. Robbins, A. Judge, I. MacLachlan, siRNA and innate immunity, Oligonucleotides 19 (2009) 89–102.
[20] A.D. Judge, V. Sood, J.R. Shaw, D. Fang, K. McClintock, I. MacLachlan, Sequence-dependent stimulation of the mammalian innate immune response by synthetic siRNA, Nat. Biotechnol. 23 (2005) 457–462.
[21] T.M. Allen, P. Sapra, E. Moase, Use of the post-insertion method for the formation of ligand-coupled liposomes, Cell. Mol. Biol. Lett. 7 (2002) 889–894.
[22] G.R. Bartlett, Colorimetric assay methods for free and phosphorylated glyceric acids, J. Biol. Chem. 234 (1959) 469–471.
[23] M. Yamauchi, H. Kusano, E. Saito, T. Iwata, M. Nakakura, Y. Kato, T. Uochi, S. Akinaga, N. Aoki, Improved formulations of antisense oligodeoxynucleotides using wrapped liposomes, J. Control. Release 114 (2006) 268–275.
[24] T. Tagami, K. Nakamura, T. Shimizu, N. Yamazaki, T. Ishida, H. Kiwada, CpG motifs in pDNA-sequences increase anti-PEG IgM production induced by PEG-coated pDNA-lipoplexes, J. Control. Release 142 (2010) 160–166.
[25] A.D. Judge, G. Bola, A.C. Lee, I. MacLachlan, Design of noninflammatory synthetic siRNA mediating potent gene silencing in vivo, Mol. Ther. 13 (2006) 494–505.
[26] L. Cekaite, G. Furset, E. Hovig, M. Sioud, Gene expression analysis in blood cells in response to unmodified and 2′-modified siRNAs reveals TLR-dependent and independent effects, J. Mol. Biol. 365 (2007) 90–108.
[27] M. Robbins, A. Judge, L. Liang, K. McClintock, E. Yaworski, I. MacLachlan, 2′-O-methyl-modified RNAs act as TLR7 antagonists, Mol. Ther. 15 (2007) 1663–1669.
[28] D.M. Klinman, A.K. Yi, S.L. Beaucage, J. Conover, A.M. Krieg, CpG motifs present in bacteria DNA rapidly induce lymphocytes to secrete interleukin 6, interleukin 12, and interferon gamma, Proc. Natl Acad. Sci. USA 93 (1996) 2879–2883.
[29] H. Hemmi, O. Takeuchi, T. Kawai, T. Kaisho, S. Sato, H. Sanjo, M. Matsumoto, K. Hoshino, H. Wagner, K. Takeda, S. Akira, A Toll-like receptor recognizes bacterial DNA, Nature 408 (2000) 740–745.
[30] F. Heil, H. Hemmi, H. Hochrein, F. Ampenberger, C. Kirschning, S. Akira, G. Lipford, H. Wagner, S. Bauer, Species-specific recognition of single-stranded RNA via toll-like receptor 7 and 8, Science 303 (2004) 1526–1529.
[31] S.S. Diebold, T. Kaisho, H. Hemmi, S. Akira, C. Reis e Sousa, Innate antiviral responses by means of TLR7-mediated recognition of single-stranded RNA, Science 303 (2004) 1529–1531.
[32] M. Sioud, Induction of inflammatory cytokines and interferon responses by double-stranded and single-stranded siRNAs is sequence-dependent and requires endosomal localization, J. Mol. Biol. 348 (2005) 1079–1090.
[33] Y.C. Tseng, L. Huang, Self-assembled lipid nanomedicines for siRNA tumor targeting, J. Biomed. Nanotechnol. 5 (2009) 351–363.
[34] S.C. Semple, A. Akinc, J. Chen, A.P. Sandhu, B.L. Mui, C.K. Cho, D.W. Sah, D. Stebbing, E.J. Crosley, E. Yaworski, I.M. Hafez, J.R. Dorkin, J. Qin, K. Lam, K.G. Rajeev, K.F. Wong, L.B. Jeffs, L. Nechev, M.L. Eisenhardt, M. Jayaraman, M. Kazem, M.A. Maier, M. Srinivasulu, M.J. Weinstein, Q. Chen, R. Alvarez, S.A. Barros, S. De, S.K. Klimuk, T. Borland, V. Kosovrasti, W.L. Cantley, Y.K. Tam, M. Manoharan, M.A. Ciufolini, M.A. Tracy, A. de Fougerolles, I. MacLachlan, P.R. Cullis, T.D. Madden, M.J. Hope, Rational design of cationic lipids for siRNA delivery, Nat. Biotechnol. 28 (2010) 172–176.
[35] T.S. Zimmermann, A.C. Lee, A. Akinc, B. Bramlage, D. Bumcrot, M.N. Fedoruk, J. Harborth, J.A. Heyes, L.B. Jeffs, M. John, A.D. Judge, K. Lam, K. McClintock, L.V. Nechev, L.R. Palmer, T. Racie, I. Rohl, S. Seiffert, S. Shanmugam, V. Sood, J. Soutschek, I. Toudjarska, A.J. Wheat, E. Yaworski, W. Zedalis, V. Koteliansky, M. Manoharan, H.P. Vornlocher, I. MacLachlan, RNAi-mediated gene silencing in non-human primates, Nature 441 (2006) 111–114.
[36] T.P. Prakash, C.R. Allerson, P. Dande, T.A. Vickers, N. Sioufi, R. Jarres, B.F. Baker, E.E. Swayze, R.H. Griffey, B. Bhat, Positional effect of chemical modifications on short interference RNA activity in mammalian cells, J. Med. Chem. 48 (2005) 4247–4253.
[37] Y.L. Chiu, T.M. Rana, siRNA function in RNAi: a chemical modification analysis, Rna 9 (2003) 1034–1048.
[38] J. Elmen, H. Thonberg, K. Ljungberg, M. Frieden, M. Westergaard, Y. Xu, B. Wahren, Z. Liang, H. Orum, T. Koch, C. Wahlestedt, Locked nucleic acid (LNA) mediated improvements in siRNA stability and functionality, Nucleic Acids Res. 33 (2005) 439–447.
[39] M.C. Glaum, S. Narula, D. Song, Y. Zheng, A.L. Anderson, C.H. Pletcher, A.I. Levinson, Toll-like receptor 7-induced naive human B-cell differentiation and immunoglobulin production, J. Allergy Clin. Immunol. 123 (2009) 224–230, e224.
[40] J.A. Hanten, J.P. Vasilakos, C.L. Riter, L. Neys, K.E. Lipson, S.S. Alkan, W. Birmachu, Comparison of human B cell activation by TLR7 and TLR9 agonists, BMC Immunol. 9 (2008) 39.
[41] A.K. Yi, J.H. Chace, J.S. Cowdery, A.M. Krieg, IFN-gamma promotes IL-6 and IgM secretion in response to CpG motifs in bacterial DNA and oligodeoxynucleotides, J. Immunol. 156 (1996) 558–564.

International Journal of Pharmaceutics 410 (2011) 153–160

Contents lists available at ScienceDirect

International Journal of Pharmaceutics

journal homepage: www.elsevier.com/locate/ijpharm

Pharmaceutical nanotechnology

# Agitation during lipoplex formation improves the gene knockdown effect of siRNA

Jose Mario Barichello[a,d,1], Shinji Kizuki[a,2], Tatsuaki Tagami[a], Tomohiro Asai[b], Tatsuhiro Ishida[a,*], Hiroshi Kikuchi[c], Naoto Oku[b], Hiroshi Kiwada[a]

[a] Department of Pharmacokinetics and Biopharmaceutics, Institute of Health Biosciences, The University of Tokushima, 1-78-1 Sho-machi, Tokushima, Japan
[b] Department of Medical Biochemistry and Global COE, Graduate School of Pharmaceutical Sciences, University of Shizuoka, Shizuoka, Japan
[c] Eisai Co., Ltd., Tokyo, Japan
[d] Japan Association for the Advancement of Medical Equipment, Tokyo, Japan

ARTICLE INFO

*Article history:*
Received 15 December 2010
Received in revised form 17 February 2011
Accepted 2 March 2011
Available online 8 March 2011

*Keywords:*
siRNA
Cationic liposome
Complex formation
Gene silencing
Vortex-mixing

ABSTRACT

The successful delivery of therapeutic siRNA to the designated target cells and their availability at the intracellular site of action are crucial requirements for successful RNAi therapy. In the present study, we focused on the siRNA-lipoplex preparation procedure and its effect on the gene-knockdown efficiency of siRNA *in vitro*. Agitation (vortex-mixing) during siRNA-lipoplex (vor-LTsiR) preparation and its effect on the gene-knockdown efficiency of stably expressed cell GFP was investigated, and their efficiency was compared with that of spontaneously formed lipoplex (spo-LTsiR). A dramatic difference in size between lipoplexes was observed at the N/P ratio of 7.62 (siRNA dose of 30 nM), even though both lipoplexes were positively charged. With the siRNA dose of 30 nM, vor-LTsiR accomplished a 50% gene-knockdown, while spo-LTsiR managed a similar knockdown effect at the 120 nM level, suggesting that the preparation procedure remarkably affects the gene-knockdown efficacy of siRNA. The uptake of vor-LTsiR was mainly via clathrin-mediated endocytosis, whereas that of spo-LTsiR was via membrane fusion. In addition, by inhibiting clathrin-mediated endocytosis, the gene-knockdown efficiency was significantly lowered. The size of the lipoplex, promoted by the preparation procedure, is likely to define the entry pathway, resulting in an increased amount of siRNA internalized in cells and an enhanced gene-knockdown efficacy. The results of the present study definitively show that a proper siRNA-lipoplex preparation procedure makes a significant contribution to the efficiency of cellular uptake, and thereby, to the gene-knockdown efficiency of siRNA.



## 1. Introduction

RNA interference (RNAi), a naturally occurring biological process of gene regulation conserved in mammalian cells (Elbashir et al., 2001), has recently shown great potential as a novel therapeutic strategy (Li et al., 2006; Behlke, 2006). The target sites of the negatively charged small interfering RNA (siRNA) used in RNAi therapy are inside the cytoplasm. Therefore, it is essential that these molecules traverse the plasma membrane to reach their target sites (Li et al., 2006; Behlke, 2006). The plasma membrane of living cells is a dynamic structure that is relatively lipophilic and negatively charged in nature, and it restricts the entry of large, hydrophilic, or negatively charged, molecules (Leung and Whittaker, 2005). Thus, an appropriate delivery system is required to achieve an efficient cellular uptake and to release the siRNA inside the cell, cytoplasm (Soutschek et al., 2004; Leung and Whittaker, 2005).

Several delivery methodologies based on viral and nonviral vectors have been developed to circumvent this problem and have been successfully used for the introduction of siRNA into cells both *in vitro* and *in vivo* (Leung and Whittaker, 2005; Li et al., 2006; Behlke, 2006). Among these methodologies, cationic liposome has shown simplicity of use and ease of large-scale production, which makes it particularly promising and potentially useful for the delivery of siRNA (Behlke, 2006; Khalil et al., 2006a). The current cationic liposomes used for siRNA delivery have been adapted from those developed to deliver plasmid DNA (pDNA) and oligodeoxynucleotide to cells. Thus, conventional siRNA-lipoplex is formed through the spontaneous electrostatic interaction between the positively charged lipid in the liposome membrane and the negatively charged phosphate backbone of the siRNA (Lasic and Templeton, 1996). Despite a certain degree of success, spontaneous

* Corresponding author. Tel.: +81 88 633 7260; fax: +81 88 633 7260.
*E-mail address:* ishida@ph.tokushima-u.ac.jp (T. Ishida).
[1] Current address: Laboratory of Nanotechnology, School of Pharmacy, Universidade Federal de Ouro Preto (UFOP), 35400-000, Ouro Preto, MG, Brazil.
[2] Co-first author.

0378-5173/$ – see front matter © 2011 Elsevier B.V. All rights reserved.
doi:10.1016/j.ijpharm.2011.03.001

formation is a static method that allows little control over the interaction process, leading to a very heterogeneous lipoplex size distribution and to excessive size (Lasic and Templeton, 1996; Kawakami et al., 2002; Faneca et al., 2004). However, although some data demonstrating the gene-knockdown efficiency of siRNA-lipoplex has been accumulated, little is known about the effect of varying the condition during lipoplex formation and to what extent this affects the gene knockdown efficiency of siRNA.

Therefore, in the present study, we focused on the preparation procedure for siRNA-lipoplex. The effect of agitation (vortexing) during siRNA-lipoplex formation on the knockdown efficiency against green fluorescence protein (GFP) stably expressed in HT-1080 cells was investigated. Also, the size distribution of lipoplex, its attached amount of siRNA, and its uptake mechanism were investigated, along with the amount of siRNA internalized in cells. Herein, we show that the uptake and promoting pathway of siRNA-lipoplex, which is modulated by the preparation procedure, influences the gene-knockdown efficiency of siRNA *in vitro*.

## 2. Material and methods

### 2.1. Materials

The cationic liposome, LipoTrust™-SR (LT), composed of *O,O'*-ditetradecanoyl-*N*-(α-trimethyl ammonioacetyl) diethanolamine chloride (DC-6-14), dioleoylphosphatidylethanolamine (DOPE) and cholesterol in the molar ratio of 1.00/0.75/0.75 was purchased from Hokkaido System Science (Hokkaido, Japan). The Hoechst 33342 was purchased from Molecular Probes (OR, USA). Z-Phe-Phe-Gly (ZfFG) and filipin complex were purchased from Sigma–Aldrich (MO, USA). The 1% Lissamine™ rhodamine B 1,2-dihexadecanoyl-sn-glycero-3-phosphoethanolamine-containing LipoTrust™-SR (RhLT) was a generous gift from Daiichi-Sankyo Pharmaceutical (Tokyo, Japan). All other chemicals were reagent grade and used as received.

### 2.2. siRNA preparation

All RNA sequences were chemically synthesized and purified with HPLC by Hokkaido System Science. The siRNA for GFP (siGFP) composed of the sense strand 5′-GGCUACGUCCAGGAGCGCACC-3′ and the antisense strand 5′-UGCGCUCCUGGACGUAGCCUU-3′ (Song et al., 2003) and the siRNA against firefly luciferase (siLuc) composed of a sense strand 5′-AGCUUCAUAAGGCGCAUGCTT-3′ and an antisense strand 5′TTUCGAAGUAUUCCGCGUACG-3′ were used as the control siRNA (Elbashir et al., 2001). The siGFP labeled at the 5′-end of the sense strand with carboxyfluorescein (FAM) (siFAM) and labeled at the 5′ end of the antisense strand with alexa Fluor 488 (siALEXA) were used as fluorescent siRNA probes, respectively. For siRNA preparation, the complementary antisense and sense strands were mixed in TE buffer ($1 \times 10^{-2}$ mM Tris–HCl, $1 \times 10^{-3}$ mM EDTA, pH 8.0, DNase and RNase free grade, Nippon Gene, Tokyo, Japan) in a 1:1 molar ratio followed by heating at 95 °C for 1 min. The reaction was then allowed to cool at room temperature. The quality of siRNA was checked by 15% PAGE. The final concentration of the duplexes was 50 μM in TE buffer.

### 2.3. Preparation of siRNA lipoplexes

Various aliquots (0.1875–6.000 μl) of the siRNA solution (50 μM) were diluted to a final volume of 100 μl with fresh Opti-MEM (Invitrogen, CA, USA). A 25 μl aliquot of LT suspension (2.4 mM) was also diluted to a final volume of 100 μl with fresh Opti-MEM. The diluted siRNA solutions were then mixed with the diluted LT suspension. The N/P ratios were set at 1.90, 3.81, 7.62, 15.24, or 30.45. The LT-siRNA lipoplexes (LTsiR) were allowed to form in two ways: the lipoplex was formed spontaneously (spo-LTsiR) by standing samples for 10 min, and the lipoplex was formed under application of a high vortex-mixing (2500 rpm) (vor-LTsiR) (Vortex-Genie 2, Scientific Industries, NY, USA) for 10 min.

### 2.4. Particle size and zeta potential of siRNA lipoplexes

The particle size and zeta-potential of siRNA lipoplexes formed at the N/P ratio of 7.62 (9.6 μM/30 nM of cationic lipid/siRNA, respectively) were determined on a Nicomp 380 Submicron Particle Sizer (Particle Sizing System, CA, USA). To determine the particle size, LTsiR lipoplexes (200 μl) were prepared in either Opti-MEM or 9% sucrose, as described above, and were diluted with 200 μl of the same medium (Opti-MEM or 9% sucrose). The mean particle size represents the average of three different preparations of the same lipoplex. For zeta-potential determination, lipoplexes were formed in 9% sucrose, and the volume was adjusted with the same medium to 2.2 ml. The zeta potential represents the average of three different preparations of the same lipoplex. Zeta-potential could not be determined in Opti-MEM due to the large amount of salts this medium contains.

### 2.5. Correlation between the relative size of the siRNA lipoplex and the amount of siRNA attached to the lipoplexes

To examine the correlation between the relative size of the siRNA lipoplex and the amount of siRNA attached to the lipoplex, LT-siFAM lipoplexes (200 μl) were prepared at an N/P ratio of 7.62 (9.6 μM/30 nM per well), as described above in Opti-MEM. Then, a flow cytometer Guava EasyCyte mini system (Guava Technology, CA, USA) equipped with an argon laser exciting at a wavelength of 488 nm was used to analyze 20,000 lipoplexes. Forward scatter and fluorescence emission was centered at 525 nm (Green fluorescence). The fluorescence was collected using a logarithmic scale. Data were analyzed using WinMDI 2.7 software (Scripps Institute, CA, USA).

### 2.6. Cells and cell culture

A human fibrosarcoma (HT-1080) cell line was purchased from Dainippon-Sumitomo Pharmaceutical (Osaka, Japan). The stably expressed green fluorescence protein (GFP) in HT-1080 cells (HT-1080GFP) was established previously by Drs. T. Asai and N. Oku (Department of Medical Biochemistry, School of Pharmaceutical Sciences, University of Shizuoka, Japan) (Yamakawa et al., 2000). The cells were cultured in DMEM (Sigma, St. Louis, MO, USA) and supplemented with 10% (v/v) heat-inactivated fetal bovine serum (FBS) (Bioserum, Tokyo, Japan), 100 IU/ml penicillin and 100 μg/ml streptomycin (ICN Biomedical, OH, USA) at 37 °C in a humidified atmosphere of 5% $CO_2$/95% air. Cells were maintained in exponential growth.

### 2.7. In vitro GFP gene knockdown

HT-1080GFP cells were seeded in 24-well plates at a density of $1.25 \times 10^4$ cells/well 24 h prior to siRNA lipofection. For lipofection, the amount of the lipoplex was fixed at 9.6 μM per well while the siRNA amounts were varied at 7.5, 15, 30, 60, and 120 nM per well. The growth medium was removed and replaced with 410 μl of Opti-MEM, 50 μl of FBS and 40 μl of LT-siGFP or LT-siLuc, followed by incubation for 24 h. Then, the medium was replaced with 500 μl of fresh DMEM containing 10% FBS and the cells again were incubated for another 24 h. To assess gene knockdown efficiency, HT-1080GFP cells were lysed in 2% Triton X-100 in PBS (100 μl/well) for 1 h on ice, following removal of the incubation media. Plates were then gently agitated in a shaker for 10 min

and 1 ml of PBS/well was added. The samples were transferred to microtubes and centrifuged at 10,000 rpm for 5 min at 4 °C. The fluorescence of the GFP in the clear lysates was measured using a standard fluorimetric method for GFP (excitation at 495 nm and emission at 510 nm) in a F-4500 Fluorescence Spectrophotometer (HITACHI, Tokyo, Japan).

### 2.8. Confocal microscopy

HT-1080 cells were seeded in a 35-mm glass-bottom dish (Iwaki Glass, Tokyo, Japan) at a density of $5 \times 10^3$ cells/dish and incubated for 24 h. For lipofection, the growth medium was replaced with 164 μl of Opti-MEM, 20 μl of FBS and 16 μl of RhLT-siFAM at the N/P ratio of 7.62 (LT/siFAM = 9.6 μM/30 nM) per well. Cells were then incubated for 4 h with RhLT-siFAM in OptiMEM. After lipofection, the cells were washed with 200 μl of PBS and then were incubated with Hoechst 33342 DMEM (10 μM) supplemented with 10% FBS for 20 min at room temperature. Confocal images were acquired using a Zeiss LSM5 inverted confocal laser scanning microscope (Carl Zeiss, Oberkochen, Germany) without fixation. LSM510 (Version 3.2 SP2) software was used to process and analyze the images.

### 2.9. Interaction and internalization of siRNA lipoplexes with cells

To investigate the cellular association and internalization of both vor-LTsiR and spo-LTsiR in HT-1080 cells, RhLT-siGFP and LT-siFAM were prepared spontaneously or with high-vortex mixing at an N/P ratio of 7.62 (9.6 μM/30 nM, respectively). HT-1080 cells were seeded at a density of $5.0 \times 10^4$ cells/well in 6-well plates and were incubated for 24 h at 37 °C. After 4 h of lipofection with LTsiR, the lipoplexes were removed and the cells were washed twice with PBS. Then, the cells were trypsinized and collected in a 1.5 ml tube. After removal of the supernatant by centrifugation (1,000 rpm, 5 min, 4 °C), the cell pellet was resuspended in 0.5 mM EDTA-PBS. The total fluorescence intensity of siRNA lipoplexes (surface-bound and internalized ones) in a cell was directly analyzed in a flow cytometer Guava EasyCyte mini system. The fluorescence intensity-related to the internalized lipoplex was analyzed after quenching the extracellular fluorescence by incubating the cells in a 0.3% trypan blue PBS solution (Zuhorn et al., 2002).

### 2.10. The uptake mechanism of siRNA lipoplexes

To examine the uptake mechanism of vor-LTsiR and spo-LTsiR by cells, the effect of the following uptake inhibitors on the internalization of the lipoplexes was investigated: a hypertonic sucrose medium, which can inhibit clathrin-mediated endocytosis through dissociation of the clathrin lattice; amiloride, which can specifically inhibit macropinocytosis by inhibiting the $Na^+/H^+$ exchange required for macropinocytosis; filipin complex, which can specifically inhibit caveolar uptake through cholesterol depletion; and, the tri-peptide ZfFG, which can inhibit membrane fusion (Khalil et al., 2006a,b). Cells were incubated with Opti-MEM supplemented with 10% FBS in the absence or presence of the inhibitors for 30 min: sucrose (0.45 M), ZfFG (200 μM), amiloride (0.5 mM), or filipin complex (5 μg/ml). LT-siFAM lipoplex (LT/siFAM = 7.2 μM/22.5 nM) was then added, followed by incubation for 1 h. The cells then were trypsinized, centrifuged at 1,000 rpm for 5 min and 4 °C, and collected in 0.3% trypan blue PBS solution to quench the extracellular fluorescence (Zuhorn et al., 2002). Trypan blue-treated cells were then washed twice with PBS, and resuspended in 0.5 mM EDTA-PBS. Samples (5,000 cells) were analyzed in a flow cytometer Guava EasyCyte mini system.

### 2.11. Influence of the uptake pathway on the gene knockdown effect of siRNA

This experiment was designed to examine the influence of the uptake pathway on the gene knockdown effect of siRNA. In this experiment, an exogenous gene instead of an endogenous gene model was used in order to shortening the time for siRNA transfection, since some of the inhibitors we used are toxic for the cell, and could lead to cell death. HT-1080 cells were seeded in a 12-well plate at a density of $2.5 \times 10^4$ cells/well in DMEM supplemented with 10% FBS prior to the experiment, then were cultured for 24 h at 37 °C. One microgram of pDNA (pEGFP-N1 vector) was transfected for 1 h with 2 μl of LipofectAMINE 2000 (Lf 2000, Invitrogen, CA, USA), according to the manufacturer's instruction. The transfection medium was then replaced with DMEM supplemented with 10% FBS and incubated for 30 min at 37 °C. After removal of the medium, the cells were incubated with OptiMEM supplemented with 10% FBS in the absence or presence of the uptake inhibitors sucrose (0.45 M), amiloride (0.5 mM), and ZfFG (200 μM) for 30 min at 37 °C. After removal of the medium, the cells were transfected with LT-siGFP or LT-siLuc (LT/siRNA = 4.8 μM/15 nM) for 2 h. The lipofection medium was then removed and replaced with fresh DMEM containing 10% FBS, and cells were incubated for a further 42 h. The cells were trypsinized, transferred to a 1.5 ml tube and centrifuged at 100 × *g* for 5 min at 4 °C. The collected cells were resuspended in 0.5 mM EDTA-PBS. A flow cytometer Guava EasyCyte mini system was then used to analyze 5,000 cells in each sample.

### 2.12. Statistical analysis

Statistical analyses (Unpaired *t*-test with Welch correction) were performed using Graph Pad Stat View software (Abacus Concepts, Inc., CA). For the GFP gene silencing effect data, a non-parametric ANOVA (Kruskal–Wallis test) with post hoc Dunn's multiple comparisons was applied using the same software. The level of significance was set at $p < 0.05$.

## 3. Results

### 3.1. The effect of agitation (vortexing) on the gene knockdown efficiency of siRNA

A different method to achieve knockdown efficiency of the GFP gene in an HT-1080GFP cell was investigated during lipoplex formation. For spo-LTsiR, an effective gene knockdown was observed at the higher dose of 120 nM of siRNA (Fig. 1A). Interestingly, for vor-LTsiR, prepared by applying vortex-mixing during lipoplex formation, a significant gene knockdown effect was observed at a dose of only 30 nM of siRNA (Fig. 1B). Alteration of the viability of HT-1080GFP cells after lipoplex treatment was not observed for any siRNA concentration we tested (data not shown). These indicate that application of agitation during lipoplex formation effectively improves the gene knockdown efficiency of siRNA.

### 3.2. Particle size and zeta-potential of siRNA lipoplexes

The mean particle size and the zeta-potential of vor-LTsiR and spo-LTsiR are summarized in Table 1. The mean sizes for the lipoplexes vor-LTsiR and spo-LTsiR when prepared in 9% sucrose were $0.300 \pm 0.045$ and $0.270 \pm 0.008$ μm, respectively. The zeta-potential of lipoplexes prepared in the same medium was $22.4 \pm 3.9$ and $18.5 \pm 0.4$ for vor-LTsiR and spo-LTsiR, respectively. In both cases, no significant difference was observed between the preparation procedures. On the other hand, when lipoplexes were formed in OptiMEM, the transfection medium that contains counter ions, there was an abrupt increase in the population of larger

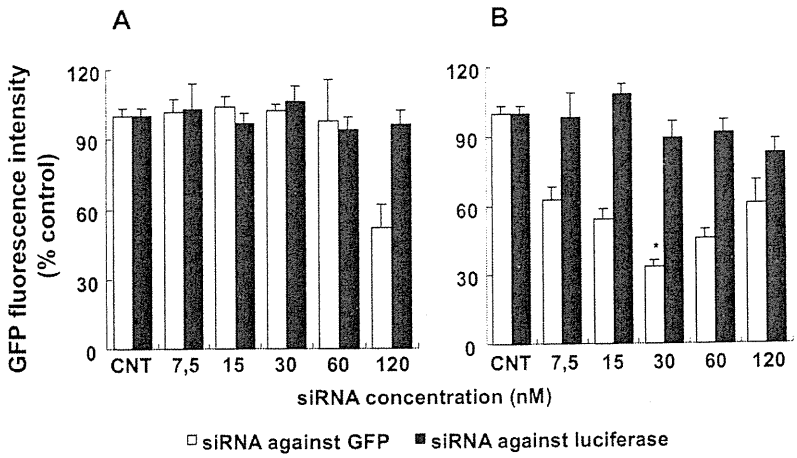


**Fig. 1.** Effect of siRNA-lipoplex preparation method on gene knockdown efficiency. (A) Lipoplex formed spontaneously (spo-LTsiR) and (B) lipoplex formed under agitation (vortex-mixing) (vor-LTsiR). Amount of cationic liposome was fixed at 9.6 μM while the N/P charge ratios were changed at 15.24, 7.62, 3.81, 1.90 and 0.95 corresponding to siRNA doses. *Legend:* CNT, control (untreated cells). *$P < 0.05$, significant difference in the mean knockdown effect of vor-LTsiR compared to spo-LTsiR at an siRNA dose of 120 nM.

lipoplexes for spo-LTsiR ($p < 0.001$). It appears that lipoplex formation under vortex-mixing allows control over the association process of cationic liposome with siRNA, leading to lipoplexes of less aggregative properties than those formed spontaneously.

### 3.3. Correlation between the size of siRNA lipoplex and the amount of siRNA attached to it

Despite the wide distribution of particle size, the preparation procedure seems to induce siRNA association to lipoplex populations of a distinct size. In vor-LTsiR (Fig. 2A), the fluorescence intensity of siRNA was detected in a narrow population of small lipoplexes (30–400 nm), indicating that each lipoplex contains a similar amount of associated siRNA. However, in spo-LTsiR (Fig. 2B), the fluorescence of siRNA was detected in relatively larger lipoplexes (150–1500 nm). Interestingly, in spo-LTsiR, the siRNA fluorescence increased in proportion to an increase in lipoplex size, indicating that larger lipoplexes contain larger amounts of siRNA. Agitation during lipoplex formation may somehow alter the association behavior of siRNA and cationic liposomes, resulting in lipoplexes that are homogeneous in terms of size distribution and amount of associated siRNA.

### 3.4. The effect of agitation (vortexing) on the internalization of lipoplexes

The cellular association of both vor-LTsiR and spo-LTsiR in HT-1080 cells was visualized by confocal microscopy (Fig. 3). Both lipoplexes were internalized, and the green fluorescence related to siRNA was co-localized with the red fluorescence related to the LT. In addition, the red fluorescence of the LT internalized in the cells was proportional between the lipoplexes, whereas the green fluorescence of the siRNA was more intense from the cells treated with vor-LTsiR than from those treated with spo-LTsiR. In addition, the amount of siRNA associated and internalized in the cells was evaluated by flow cytometry (Fig. 4). In spite of the LT and siRNA, the total (surface-bound + internalized) fluorescence intensity in the cells was comparable between vor-LTsiR and spo-LTsiR. In the internalized fraction of lipoplexes, the fluorescence intensity of the LT was also comparable between lipoplexes, while that of the siRNA was 3-fold higher for vor-LTsiR in comparison with spo-LTsiR. These findings indicate that a large amount of siRNA transfected with the spo-LTsiR simply was associated with the cellular surface, and was not being internalized in the cells.

**Table 1**
Effect of the lipoplex formation method on particle size and zeta potential of the siRNA lipoplex.

| | Size | | Zeta-potential (mV) |
|---|---|---|---|
| | Opti-MEM (μm) | Sucrose 9% (μm) | |
| LTrust alone | 0.233 ± 0.006 | 0.239 ± 0.003 | 21.6 ± 2.0 |
| spo-LTsiR | 8.290 ± 1.560 | 0.270 ± 0.008 | 18.5 ± 0.4 |
| vor-LTsiR | 2.040 ± 0.500* | 0.300 ± 0.045 | 22.4 ± 3.9 |

The cationic liposome/siRNA ratio was 9.6 μM/30.0 nM and corresponds to an N/P ratio of 7.62. The data represent the mean ± S.D. of three independent experiments performed in triplicate.

* $P < 0.001$, significant difference between the mean particle size of vor-LTsiR and spo-LTsiR.

### 3.5. The uptake mechanism of siRNA transfected by cell lipoplexes

The internalization pathways of both vor-LTsiR and spo-LTsiR were evaluated as an indication of fluorescence intensity for siRNA in the presence of various inhibitors (Fig. 5). The uptake of vor-LTsiR was inhibited at around 42% by the 0.45 M sucrose (clathrin-mediated endocytosis inhibitor), 22% by the ZfFG (fusion inhibitor), and 22% by the amiloride (macropinocytosis inhibitor). The uptake of spo-LTsiR was inhibited 16% by 0.45 M sucrose, 45% by ZfFG, and 22% by amiloride. The treatment with filipin complex (caveolae-mediated endocytosis inhibitor) did not inhibit the uptake of either lipoplex. These results clearly indicate that vor-LTsiR is mainly internalized via clathrin-mediated endocytosis, whereas spo-LTsiR is mainly internalized through membrane fusion.

### 3.6. Effect of the uptake pathway on the gene knockdown efficiency of vor-LTsiR

The contribution of each uptake pathway of vor-LTsiR to the gene knockdown effect was evaluated (Fig. 6). The knockdown efficiency of the GFP gene was inhibited 25.7 ± 3.5% by 0.45 M sucrose (clathrin-mediated endocytosis) and 10.4 ± 2.8% by amiloride (macropinocytosis), but was not affected by the filipin complex (caveolae-mediated endocytosis inhibitor). The ZfFG, however, enhanced the knockdown efficiency of vor-LTsiR (membrane fusion). These suggest that clathrin-mediated endocytosis and macropinocytosis is the major contributing pathway of

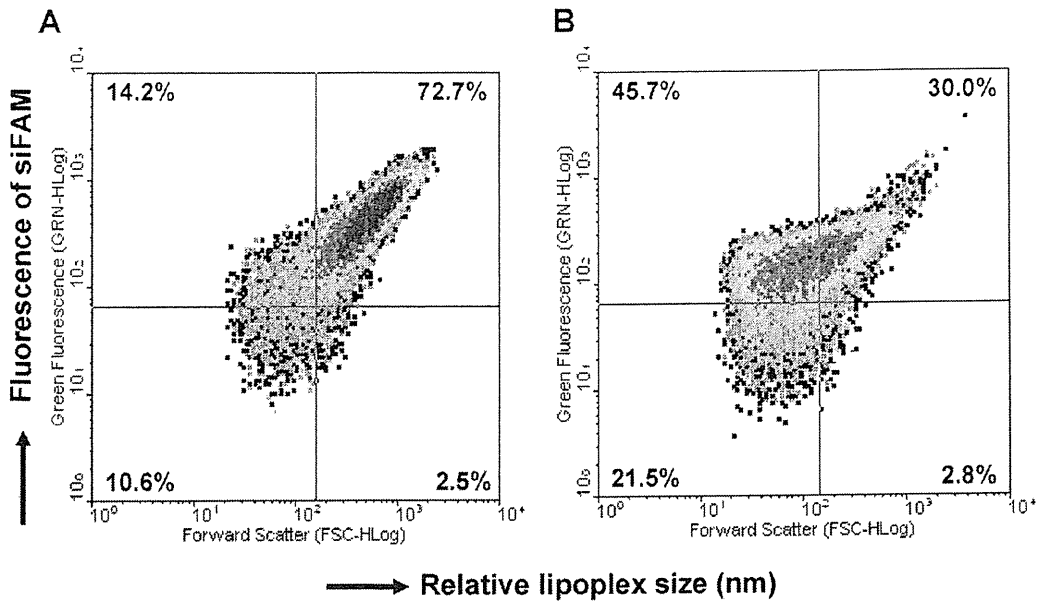


**Fig. 2.** Effect of lipoplex preparation method on siRNA-lipoplex size distribution. (A) Lipoplex formed spontaneously (spo-LTsiR) and (B) lipoplex formed under agitation (vortex-mixing) (vor-LTsiR). Cationic liposome/siRNA ratio was 9.6 μM/30.0 nM and corresponds to an N/P ratio of 7.62. The size distribution and fluorescence intensity of the lipoplexes were measured by flow cytometry.

vor-LTsiR to achieve effective gene knockdown in HT-1080GFP cells.

## 4. Discussion

siRNA lipoplex usually forms spontaneously, and allows for little control over the process of cationic liposome interaction, which leads to both a wide size distribution and excessive sizes (Lasic and Templeton, 1996; Kawakami et al., 2002; Faneca et al., 2004). In the present study, the initial focus was on investigating the effect of agitation during siRNA lipoplex formation (vor-LTsiR) on the *in vitro* knockdown efficiency of GFP gene stably expressed in HT-1080 cells. This system can partially simulate the downregulation of an endogenous gene. The present study demonstrated that vor-LTsiR could efficiently knockdown the GFP gene using a dose of siRNA against GFP that was 4-fold lower than the dose of spo-LTsiR (Fig. 1).

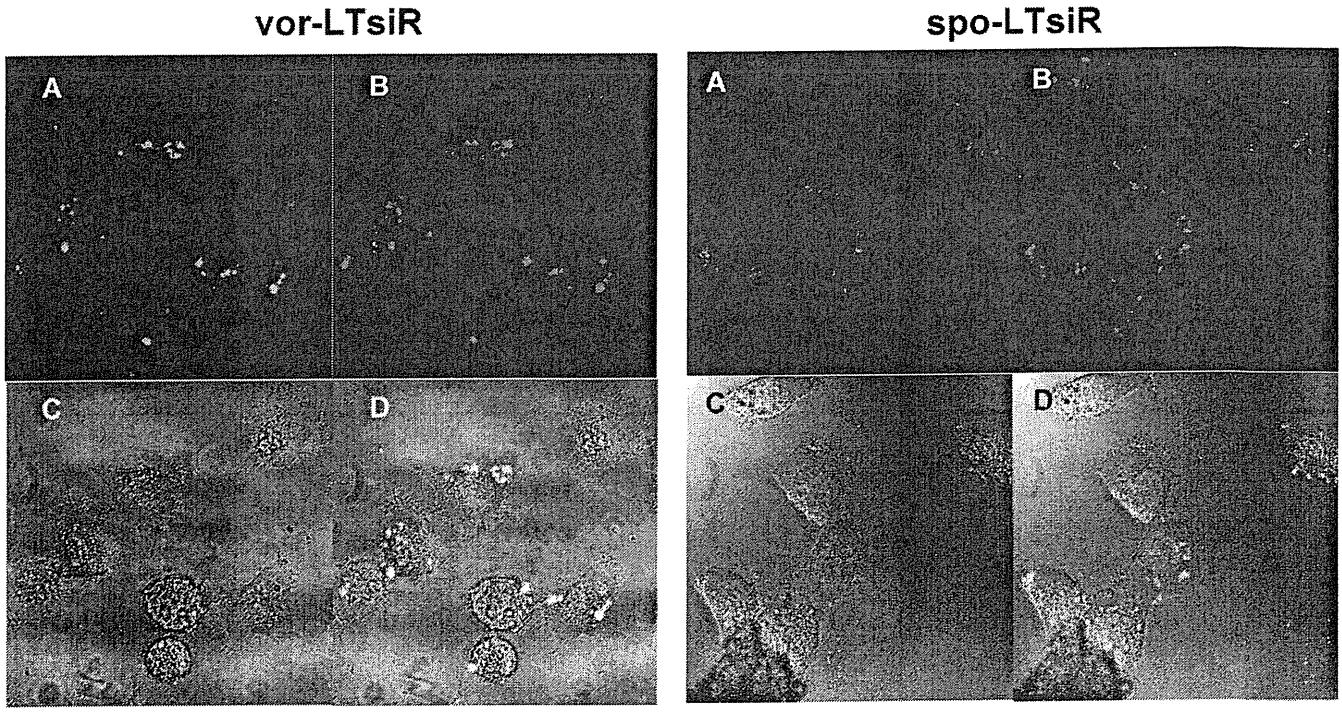


**Fig. 3.** Visualization of the intracellular vor-LTsiR (left) and spo-LTsiR (right) in the cell. Cationic liposome/siRNA amount was 9.6 μM/30.0 nM and corresponds to a charge ratio of 7.62. (A) siRNA (green), (B) LT (red), (C) phase-contrast image, and (D) merged image of A, B and C. Blue corresponds to the nucleus. (Magnification: ×630.) (For interpretation of the references to color in this figure legend, the reader is referred to the web version of this article.)

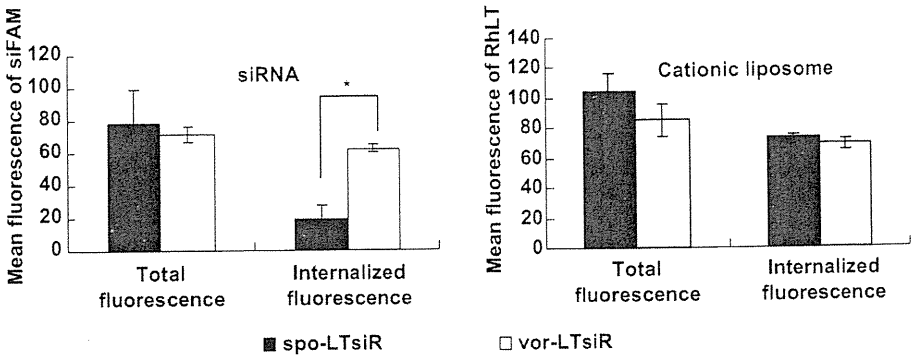


**Fig. 4.** Amount of siRNA associated with lipoplexes internalized by the cells. Total fluorescence represents the siRNA which was surface-bound and internalized in the cells. Cationic lipid/siRNA amount was 9.6 μM/30.0 nM and corresponds to an N/P ratio of 7.62. Data represent the mean ± S.D. of three independent experiments performed in triplicate. *$P < 0.05$ was considered significant.

The results of the present study clearly showed that the preparation procedure affects not only the physicochemical property of siRNA lipoplex but also their gene knockdown efficiency.

The interaction of particles with cells is significantly influenced by particle size (Rejman et al., 2004; Khalil et al., 2006b; Gratton et al., 2008) and surface charge (Lima et al., 2001). The surface charges of both lipoplexes were positive at the siRNA concentration (N/P ratio of 7.62 (9.6 μM/30 nM; $L^+/siRNA^-$)) where the most distinct difference in the RNAi effect was observed. The size of both lipoplexes did not vary significantly when prepared in 9% sucrose, a medium free of counter ions. However, when prepared in Opti-MEM, the medium most routinely used for lipofection, the lipoplexes displayed a heterogeneous size distribution (Table 1) due to the effect of counter ions that stimulate the aggregative properties of lipoplexes (Spagnou et al., 2004). The mean particle size of spo-LTsiR was at least 3-fold larger than that of vor-LTsiR. In addition, the lipoplexes prepared by different procedures displayed a very heterogeneous association of siRNA to distinct lipoplex size population. In vor-LTsiR, approximately 80% of the siRNA molecules attached to the lipoplex smaller than 200 nm, whereas in spo-LTsiR,

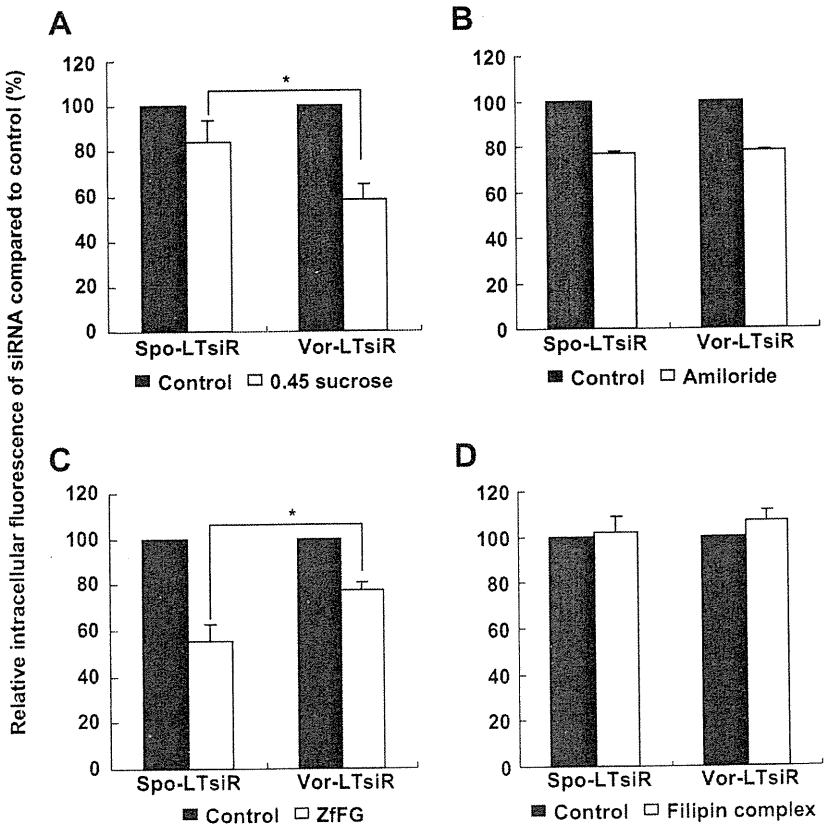


**Fig. 5.** Uptake mechanism of vor-LTsiR (left) and spo-LTsiR (right) by the cells. siRNA lipoplexes were incubated with the cells, which were treated with various uptake inhibitors. The fluorescence intensity relating to siRNA in the cells was determined by flow cytometry. Data represent the mean ± S.D. of three independent experiments performed in triplicate. *$P < 0.05$ was considered significant. Inhibition of (A) clathrin-mediated endocytosis, (B) macropinocytosis, (C) membrane fusion, and (D) caveolae-mediated endocytosis.

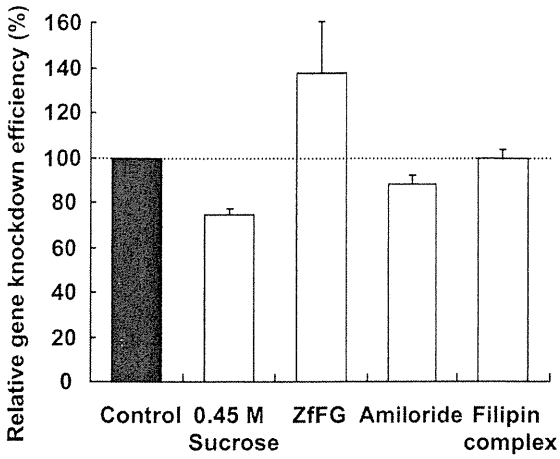


**Fig. 6.** The major uptake route contributing to the gene knockdown effect of vor-LTsiR. Data represent the mean ± S.D. of three independent experiments performed in triplicate. Cells were transfected with vor-LTsiR in the absence (control) or in the presence of sucrose, ZfFG, amiloride or filipin complex. GFP fluorescence was measured at 22 h after transfection by flow cytometry.

only around 36% of the siRNA attached to a relative lipoplex size (Fig. 2). Given the same lipid concentration, a smaller lipoplex size would equate to a larger total surface area. A larger total surface area for lipoplex can promote extensive interactions with target cells. Hence, the higher gene knockdown efficiency induced by vor-LTsiR at a relatively lower siRNA dose (Fig. 1) might be due to the efficient delivery of siRNA into the cells as a result of the enhanced interaction of the lipoplex with the cells. This assumption is strongly supported by the results of qualitative and quantitative analysis, as described in Figs. 3 and 4.

From the mechanism of RNAi, the intracellular presence of siRNA molecules complementary to the target mRNA is of crucial importance for inducing gene knockdown (Behlke, 2006; Li et al., 2006). Therefore, it is essential that the siRNA lipoplex is taken up intact by the cells, and that the lipoplex efficiently releases the siRNA molecule into the cytoplasm (Khalil et al., 2006a). As shown in Fig. 3, in the vor-LTsiR, LT (red) was extensively co-localized with siRNA (green), indicating that the lipoplex associated with siRNA was efficiently internalized in the cells. In the spo-LTsiR, however, the LT (red) was less co-localized with siRNA (green), indicating either that the lipoplex were associated with fewer siRNA or that empty LT were internalized. In addition, the result of semi-quantitative evaluation (Fig. 4) indicated that vor-LTsiR improved 3-fold the amount of siRNA internalized in the cells compared with spo-LTsiR, although there was no significant difference in the total amount of siRNA and LT that interacted with the cells between both formulations. Accordingly, the superior gene knockdown efficacy of vor-LTsiR observed in Fig. 1 may be explained by the following scenario: the smaller sized (≤200 nm) vor-LTsiR contained a large amount of siRNA (Fig. 2A) and were extensively taken up by the targeted cells (Fig. 4 left). However, the smaller sized (≤200 nm) spo-LTsiR contained fewer siRNA (Fig. 2B) that were taken up by the cells and the remaining spo-LTsiR (≥200 nm) simply associated with the cell surface, which limited or delayed their internalization. Several studies have demonstrated that the uptake of viral particles (Matlin et al., 1982), polyplexes (Godbey et al., 1999), and beads (Rejman et al., 2004) by cells is delayed in a size-dependent manner.

Particle size determines the pathway of cellular entry, and therefore, also determines the kinetics of internalization and the intracellular trafficking of the particles (Rejman et al., 2004; Gratton et al., 2008). There is convincing evidence that endocytosis represents the major pathway of entry into cells for particles <1 μm in size (Rejman et al., 2004; Spagnou et al., 2004; Khalil et al., 2006a; Hoekstra et al., 2007; Gratton et al., 2008). These pathways include phagocytosis, clathrin-dependent endocytosis and clathrin-independent endocytosis, the latter including macropinocytosis and internalization via caveolae (Rejman et al., 2004; Khalil et al., 2006a; Sahay et al., 2010). In the present study, three pathways were found in the uptake of both lipoplexes by cells. As shown in Fig. 5, the internalization of vor-LTsiR was mainly via clathrin-mediated endocytosis while macropinocytosis and cell fusion were secondary routes. On the contrary, the internalization of spo-LTsiR was mainly through membrane fusion while macropinocytosis and clathrin-mediated endocytosis were secondary routes. At present, the majority of reports suggest that positively charged nanomaterials predominantly internalize through clathrin-mediated endocytosis with some fraction utilizing macropinocytosis (Sahay et al., 2010). Our current results are consistent with the previous reports.

Clathrin-mediated endocytosis and macropinocytosis have been suggested as the major routes of cellular entry for lipoplexes containing nucleic acids such as pDNA and siRNA (Thomsen et al., 2002; Zuhorn et al., 2002; Zhang et al., 2003; Nakase et al., 2004; Spagnou et al., 2004; Wadia et al., 2004; Kaplan et al., 2005; Rejman et al., 2005; Khalil et al., 2006a; Sahay et al., 2010). The present study also clearly showed that both routes are major inducements of the vor-LTsiR-mediated gene silencing effect (Fig. 6). Under normal conditions, the formation of clathrin-coated pits is very rapid (within 28 s), with the entire population of coated pits being turned over approximately every 6 min, making this structure highly mobile (Kawakami et al., 2002). Particles of 50 and 100 nm in size are internalized in a relatively rapid process by this pathway (Rejman et al., 2004). Hence, it is assumed that the lipoplex of vor-LTsiR (≤200 nm), which contains 80% siRNA, are quickly and extensively internalized (Figs. 3 and 4), resulting in an efficient gene-knockdown effect (Fig. 1). Macropinocytosis is known as an efficient route for the nonselective endocytosis of solute macromolecules and provides some advantageous aspects on siRNA-based gene-knockdown such as the avoidance of lysosomal degradation and an easing of the escape from macropinosomes (Khalil et al., 2006a). However, in the present study, it appears that macropinocytosis only partly contributes to vor-LTsiR-mediated gene silencing.

Cationic liposome, including lipoplex, is known to interact and fuse with cell membranes (Leventis and Silvius, 1990). Fusion was one of the major cellular entry routes for spo-LTsiR, which agrees with previous reports (Fig. 5). Size is known to be one of the most important factors affecting the dynamics of vesicle sedimentation onto the cells (Faneca et al., 2004). In the present study, lipoplexes formed spontaneously in Opti-MEM, the transfection medium, and presented a wider size distribution due to the relatively uncontrolled process of association between siRNA and LT. Accordingly, in spo-LTsiR, approximately 64% of siRNA preferentially attached to lipoplexes larger than 200 nm in size (Fig. 2). Assuming that spo-LTsiR (≥200 nm) is taken up only to a limited extent by macropinocytosis, the remaining lipoplexes bound to the cell surface are assumed to be held at the cell surface for a relatively longer period. Such a long period on the cell surface might lead to the progressive dilution of the lipoplexes as the cell divide (Leung and Whittaker, 2005). In addition, extensive leakage of contents from phosphatidylethanolamine-based liposomes is known to occur during fusion (Brown and Silvius, 1989). This may expose the siRNA associated with, or released from, the spo-LTsiR to potential enzymatic or physical degradation before it can reach the cytoplasm (Spagnou et al., 2004). Consequently, spo-LTsiR might have shown a lower gene knockdown effect in the present study (Fig. 1).

## 5. Conclusion

The present study showed that the preparation procedure for siRNA-lipoplex remarkably affects the *in vitro* gene-knockdown efficiency of siRNA. Smaller (≤200 nm) and relatively homogeneous lipoplexes containing a large amount of siRNA (80% of dose), produced by agitation (vortex-mixing) during the preparation, allowed for the efficient cellular interaction of lipoplex and a shift in their entry pathway from fusion to clathrin-mediated endocytosis, resulting in an increased amount of siRNA internalized in cells, and thereby, an enhanced gene-knockdown efficacy. A proper siRNA-lipoplex preparation procedure was strongly related to both the efficiency of cellular uptake and the gene-knockdown efficiency of siRNA. The results of the present study may have implications for designing a more efficient and successful siRNA delivery system.

## Acknowledgements

The authors thank Dr. James L. McDonald for his helpful advice in developing the English manuscript. This work was supported in part by the Health and Labour Sciences Research Grants for Research on Advanced Medical Technology from The Ministry of Health, Labour and Welfare of Japan. We thank the Japan Association for the Advancement of Medical Equipment for supporting a Postdoctoral Fellowship for Dr. Jose Mario Barichello.

## References

Behlke, M.A., 2006. Progress towards in vivo use of siRNAs. Mol. Ther. 13, 644–670.
Brown, P.M., Silvius, J.R., 1989. Stability and fusion of lipid vesicles containing headgroup-modified analogues of phosphatidylethanolamine. Biochim. Biophys. Acta 980, 181–190.
Elbashir, S.M., Harborth, J., Lendeckel, W., Yalcin, A., Weber, K., Tuschl, T., 2001. Duplexes of 21-nucleotide RNAs mediate RNA interference in cultured mammalian cells. Nature 411, 494–498.
Faneca, H., Simoes, S., Pedroso de Lima, M.V., 2004. Association of albumin or protamine to lipoplexes: enhancement of transfection and resistance to serum. J. Gene Med. 6, 681–692.
Godbey, W.T., Wu, K.K., Mikos, A.G., 1999. Tracking the intracellular path of poly(ethylenimine)/DNA complexes for gene delivery. Proc. Natl. Acad. Sci. U.S.A. 96, 5177–5181.
Gratton, S.E.A., Ropp, P.A., Pohlhaus, P.D., Luft, J.C., Madden, V.J., Napier, M.E., DeSimone, J.M., 2008. The effect of particle design on cellular internalization pathways. Proc. Natl. Acad. Sci. U.S.A. 105, 11613–11618.
Hoekstra, D., Rejman, J., Wasungu, L., Shi, F., Zuhorn, I., 2007. Gene delivery by cationic lipids: in and put of an endosome. Biochem. Soc. Trans. 35, 68–71.
Kaplan, I.M., Wadia, J.S., Dowdy, S.F., 2005. Cationic TAT peptide transduction domain enters cells by macropinocytosis. J Control. Release 102, 247–253.
Kawakami, S., Yamashita, F., Nishida, K., Nakamura, J., Hashida, M., 2002. Glycosilated cationic liposomes for cell-selective gene delivery. Crit. Rev. Ther. Drug Carrier Syst. 19, 171–190.
Khalil, I.A., Kogure, K., Akita, H., Harashima, H., 2006a. Uptake pathways and subsequent intracellular trafficking in nonviral gene delivery. Pharmacol. Rev. 58, 32–45.
Khalil, I.A., Kogure, K., Futaki, S., Harashima, H., 2006b. High density of octaarginine stimulates macropinocytosis leading to efficient intracellular trafficking for gene expression. J. Biol. Chem. 281, 3544–3551.
Leung, R.K.M., Whittaker, P.A., 2005. RNA interference: from gene silencing to gene-specific therapeutics. Pharmacol. Ther. 107, 222–239.
Lasic, D.D., Templeton, N.S., 1996. Liposomes in gene delivery. Adv. Drug Deliv. Rev. 20, 221–266.
Leventis, R., Silvius, J.R., 1990. Interactions of mammalian cells with lipid dispersions containing novel metabolizable cationic amphiphiles. Biochim. Biophys. Acta 1023, 124–132.
Li, C.X., Parker, A., Menocal, E., Xiang, S., Borodyansky, L., Fruehauf, J.H., 2006. Delivery of RNA interference. Cell Cycle 5, 2103–2109.
Lima, M.C.P., Simões, S., Pires, P., Faneca, H., Düzgüneş, N., 2001. Cationic lipid-DNA complexes in gene delivery: from biophysics to biological applications. Adv. Drug Deliv. Rev. 47, 277–294.
Matlin, K.S., Reggio, H., Helenius, A., Simons, K., 1982. Pathway of vesicular stomatis virus entry leading to infection. J. Mol. Biol. 156, 609–631.
Nakase, I., Niwa, M., Takeuchi, T., Sonomura, K., Kawabata, N., Koike, Y., Takehashi, M., Tanaka, S., Ueda, K., Simpson, J.C., Jones, A.T., Sugiura, Y., Futaki, S., 2004. Cellular uptake of arginine-rich peptides: roles for macropinocytosis and actin rearrangement. Mol. Ther. 10, 1011–1022.
Rejman, J., Oberle, V., Zuhorn, I.S., Hoekstra, D., 2004. Size-dependent internalization of particles via the pathways of clathrin and caveolae-mediated endocytosis. Biochem. J. 377, 159–169.
Rejman, J., Bragonzi, A., Conese, M., 2005. Role of clathrin- and caveolae-mediated endocytosis in gene transfer mediated by lipo- and polyplexes. Mol. Ther. 12, 468–474.
Sahay, G., Alakhova, D.Y., Kabanov, A.V., 2010. Endocytosis of nanomedicines. J. Control. Release 145, 182–195.
Song, E., Lee, S.-K., Dykxhoorn, D.M., Novina, C., Zhang, D., Crawford, K., Cerny, J., Sharp, P.A., Lieberman, J., Manjunath, N., et al., 2003. Sustained small interfering RNA-mediated human immunodeficiency virus type 1 inhibition in primary macrophages. J. Virol. 77, 7174–7181.
Soutschek, J., Akinc, A., Bramlage, B., Charisse, K., Constien, R., Donoghue, M., Elbashir, S., Geick, A., Hadwiger, P., Harborth, J., et al., 2004. Therapeutic silencing of an endogenous gene by systemic administration of modified siRNAs. Nature 432, 173–178.
Spagnou, S., Miller, A.D., Keller, M., 2004. Lipidic carriers of siRNA: differences in the formulation, cellular uptake, and delivery with plasmid DNA. Biochemistry 43, 13348–13356.
Thomsen, P, Roepstorff, K., Stahlhut, M., van Deurs, B., 2002. Caveolae are highly immobile plasma membrane microdomains, which are not involved in constitutive endocytic trafficking. Mol. Biol. Cell 13, 238–250.
Wadia, J.S., Stan, R.V., Dowdy, S.F., 2004. Transducible TAT-HA fusogenic peptide enhances escape of TAT-fusion proteins after lipid raft macropinocytosis. Nat. Med. 10, 310–315.
Yamakawa, S., Furuyama, Y., Oku, N., 2000. Development of a simple cell invasion assay system. Biol. Pharm. Bull. 23, 1264–1266.
Zhang, Y., Garzon-Rodriguez, W., Manning, M.C., Anchordoquy, T.J., 2003. The use of fluorescence resonance energy transfer to monitor dynamic changes of lipid-DNA interactions during lipoplex formation. Biochim. Biophys. Acta 1614, 182–192.
Zuhorn, I.S., Kalicharan, R., Hoekstra, D., 2002. Lipoplex-mediated transfection of mammalian cells occurs through the cholesterol-dependent clathrin-mediated pathway of endocytosis. J. Biol. Chem. 277, 18021–18028.

Drug Deliv. and Transl. Res. (2011) 1:277–288
DOI 10.1007/s13346-011-0025-3

RESEARCH ARTICLE

# Argonaute2 is a potential target for siRNA-based cancer therapy for HT1080 human fibrosarcoma

**Tatsuaki Tagami · Takuya Suzuki · Kiyomi Hirose · Jose Mario Barichello · Naoshi Yamazaki · Tomohiro Asai · Naoto Oku · Tatsuhiro Ishida · Hiroshi Kiwada**

Published online: 9 April 2011


**Abstract** Small interfering RNAs (siRNAs) are small RNA molecules that have a potent, sequence-specific gene silencing effect and therefore show promise for therapeutic use as molecular-targeted drugs for the treatment of various genetic diseases, including cancer. The aim of the present study was to evaluate whether Argonaute2 (Ago2) is a therapeutically effective target for siRNA-based cancer therapy. Ago2 is the key protein in mammalian RNAi and is also known as the only member of the Ago family that mediates the microRNA (miRNA)-dependent cleavage of targeted mRNAs. It is assumed that these unique properties of the Ago2 protein can play a central role in the regulation of the miRNA pathway and subsequent translational inhibition of miRNA-targeted mRNAs, including cell survival and cancer progression. To assess its therapeutic effect, siRNA against Ago2 (Ago2-siRNA) was transfected into HT1080 human fibrosarcoma cells, which are malignant cancer cells. Ago2 gene silencing resulted in the inhibition of cell growth and the induction of apoptosis and G0/G1 arrest in the cell cycle. In addition, Ago2 knockdown induced morphological changes and actin stress fiber formation in the cells. The results of a microarray study showed that Ago2 suppression stimulated several crucial genes related to apoptosis, the cell cycle, immune response, cell adhesion, metabolism, etc. Repeated intratumoral injection of Ago2-siRNA/cationic liposome complex induced tumor growth suppression in an HT1080 xenograft model. These results suggest that the suppression of the

T. Tagami · T. Suzuki · K. Hirose · J. M. Barichello · T. Ishida (✉) · H. Kiwada
Department of Pharmacokinetics and Biopharmaceutics, Subdivision of Biopharmaceutical Sciences, Institute of Health Biosciences, The University of Tokushima,
1-78-1 Sho-machi,
Tokushima 770-8505, Japan
e-mail: ishida@ph.tokushima-u.ac.jp

J. M. Barichello
Japan Association for the Advancement of Medical Equipment, Tokyo, Japan

N. Yamazaki
Department of Medicinal Biochemistry, Subdivision of Biopharmaceutical Sciences, Institute of Health Biosciences, The University of Tokushima,
Tokushima, Japan

T. Asai · N. Oku
Department of Medical Biochemistry, Graduate School of Pharmaceutical Sciences, University of Shizuoka,
Suruga-ku,
Shizuoka 422-8526, Japan

T. Asai · N. Oku
Global COE Program, University of Shizuoka,
Suruga-ku,
Shizuoka, Japan

*Present Address:*
T. Tagami
Ontario Institute for Cancer Research, MaRS Centre,
South Tower, 101 College Street, Suite 800,
Toronto, ON, Canada M5G 0A3

*Present Address:*
J. M. Barichello
Laboratory of Nanotechnology, School of Pharmacy,
Universidade Federal de Ouro Preto (UFOP),
35400-000 Ouro Preto, Minas Gerais, Brazil

Ago2 gene may be useful for the inhibition of cancer progression and that Ago2 may be a desirable target for siRNA-based cancer therapy.

**Keywords** Argonaute2 (Ago2) · Small interfering RNA (siRNA) · RNA interference (RNAi) · Fibrosarcoma · Cationic liposome

## Introduction

Fibrosarcoma is a rare malignant tumor derived from fibroblasts and is predominantly found around bone and soft tissue [1]. This tumor is associated with the abnormal disposition of collagen and other extracellular matrix components that cause invasion, after which the presence of immature blood vessels favors metastasis through the blood stream. The current treatment for inoperable fibrosarcoma is radiotherapy and chemotherapy, but the prognosis after treatment is poor [2]. A novel therapeutic modality to suppress further progression is therefore required.

RNA interference (RNAi) is a natural process that affects gene silencing in eukaryotes at the transcriptional, post-transcriptional, and/or translational levels [3]. Small interfering RNAs (siRNAs), which are short double-stranded RNA duplexes, are the key intermediates in RNAi that can potentially inhibit the expression of any targeted genes. Due to its potent, sequence-specific gene silencing effects, siRNA is a promising biological tool and potential therapeutic agent against many kinds of genetic diseases, including cancer [4]. From various points of view, many genes are seen as potential targets for siRNA-based cancer therapy. Most potential target genes for siRNA-based cancer therapy are specifically overexpressed in cancer cells, and their knockdown is less toxic to normal cells [5]. Most oncogenes have these properties, and several siRNAs against oncogenes, such as K-ras and c-myc, have shown remarkable therapeutic effects [6, 7]. Other potential target genes for siRNA therapy are those that are involved in multiple pathways or that are critical for cell survival [8]. These genes include those involved in angiogenesis (VEGF [9] and EGFR [10]), metastasis (MMPs [11]), survival (Survivin [12]), anti-apoptosis (bcl-2 [13] and XIAP [14]), resistance to chemotherapy (MDR1 [15]), and synthetic lethality (PLK1 [16] and STK33 [17]). The knockdown of these targets can effectively inhibit the many stages of cancer progression, resulting in efficient therapeutic effects. However, it is also true that familiar target genes may not be "druggable" because siRNAs against familiar genes can easily be replaced by the development of chemical inhibitors that are advantageous in molecular weight and delivery efficiency [18]. Therefore, researchers have explored the frontiers of novel target genes for siRNA-based cancer therapy.

The present study focused on the Argonaute2 (Ago2, also known as EIF2C2) gene as a novel candidate for siRNA-based cancer therapy for the following reasons: (1) Ago2 can broadly regulate both microRNAs (miRNAs) and miRNA-mediated multiple pathways, including cell survival and cancer progression. miRNAs are endogenous small RNAs that are one of the largest classes of gene regulators [19]. They regulate approximately 30% of protein-coding transcripts [20]; therefore, miRNAs control a wide range of biological processes, including cancer [21]. Some miRNAs can be oncogenic, such as the miR17-92 cluster, miR-21, etc., termed onco-miRs [22], although the function of most onco-miRs is still unclear. miRNAs are incorporated with Ago2, and then these complexes collaborate in the translational inhibition of targeted mRNAs [23]. It is therefore expected that Ago2 gene silencing can halt the development of cancer by blocking the function of miRNAs and many mRNAs regulated by miRNAs. (2) Ago2 can function as a central regulator of miRNAs. Ago2 is a member of the Ago protein family which consists of eight members in mammals [24]. Four Ago proteins are ubiquitously expressed (Ago subfamily) and the remaining four (Piwi subfamily) are expressed in germ cells. All four mammalian Ago subfamilies (Ago1 through Ago4) are associated with miRNAs, but only Ago2, which has a structure like that of RNase as a "slicer," can mediate the specific endonucleolytic cleavage of targeted mRNAs incorporated with miRNAs in mammalian cells [23, 25]. It is therefore expected that the unique and essential roles of the Ago2 gene in controlling miRNA pathways could seriously affect the survival of cancer cells. (3) As far as we know, there has been no report of severe side effects caused by inhibiting the Ago2 gene in vivo. Ago2 is a relatively well-characterized protein in the Ago family, and several reports have mentioned that Ago2 knockout is lethal to embryos because of neural tube defects [23] and defective B cell proliferation [26]. However, the shorter duration of Ago2 gene suppression induced by siRNA would not lead to such severe side effects in adult animals. For these reasons, the present study challenged Ago2 gene knockdown by transfection with siRNA against Ago2 (Ago2-siRNA) into human fibrosarcoma HT1080 cells and then characterized phenotypical changes in the cells. Global gene suppression on the mRNA level was analyzed by microarray following Ago2 gene suppression.

In addition, in this study, in vivo Ago2-siRNA delivery and antitumor effect was evaluated with a cationic liposome (TFL-3) which has been established in our previous studies [27, 28]. Cationic liposome is safer than viral vector, and its simple and easy scaling up is suitable for manufacture. Therefore, cationic liposome has been extensively investi-

gated for the delivery of nucleic acids including plasmid DNA, antisense oligonucleotide, and siRNA as translational research [13, 29–31].

## Materials and methods

### Cell culture

Human fibrosarcoma cells (HT1080) were obtained from Dainippon-Sumitomo Pharmaceutical (Osaka, Japan) and maintained in Dulbecco's modified Eagle's medium (DMEM, Nissui Pharmaceutical, Tokyo, Japan) supplemented with 10% heat-inactivated fetal bovine serum (FBS, Japan Bioserum, Hiroshima, Japan), 10 mM L-glutamine, 100 U/ml penicillin, and 100 μg/ml streptomycin (ICN Biomedical, OH, USA). Cells were incubated at 37°C in a humidified incubator atmosphere of 5% $CO_2$/95% air.

### Small interfering RNAs

siRNAs were chemically synthesized and purified through HPLC by Hokkaido System Science (Hokkaido, Japan). The sequences of siRNAs were cited from previous reports as follows: siRNA for Ago2 (Ago2-siRNA), the sequence that exhibited the highest gene silencing effect in siRNAs designed in a previous report [25] (sense sequence 5′-GCA CGGAAGUCCAUCUGAAUU-3′ and antisense sequence 5′-UUCAGAUGGACUUCCGUGCUU-3′) and control siRNA (Cont-siRNA), the sequence that was targeted for firefly luciferase [32] (sense sequence 5′-CUUACGCUGA GUACUUCGATT-3′ and antisense sequence 5′-UCGAA GUACUCAGCGUAAGTT-3′).

For the preparation of siRNA duplexes, the complementary antisense and sense strands, DNase- and RNase-free grade (Nippon Gene, Tokyo, Japan), were mixed in equal amounts in TE buffer (10 μM Tris–HCl, 1 μM EDTA, pH 8.0) followed by heating at 90°C for 1 min. The reaction mixture was then allowed to cool at room temperature. The quality of siRNA duplexes was checked by 15% polyacrylamide gel electrophoresis (PAGE). The final concentration of the duplexes was 50 μM in TE buffer.

### siRNA transfection

Cells were seeded at a density of 2,500 cells/well in a 96-well plate with 100 μl culture medium, 50,000 cells/well in a six-well plate with 2 ml, or 250,000 cells/well in a 10-cm dish with 10 ml as the experimental scale. At 24 h after seeding, the cells were transfected with the appropriate concentration of siRNA using LipofectAMINE 2000 (Lf 2000, Invitrogen, CA, USA) according to the manufacturer's instruction. Briefly, siRNA was premixed with Lf 2000 at a ratio of 1:5 (siRNA (micrograms)/Lf2000 (microliters)) in Opti-MEM I (Invitrogen) in a microtube, and the mixture was then held for 20 min at room temperature to form siRNA/Lf2000 complex. The siRNA/Lf2000 complex was applied to the wells or dishes, and the cells were then incubated in a medium containing FBS (final concentration 6.66% FBS). At 24 h post-transfection, the medium was replaced with fresh DMEM supplemented with 10% FBS, and the cells were then used for additional assays.

### Western blotting

Western blotting was carried out as previously described [33]. Briefly, cells were seeded at a density of 250,000 cells/dish in a 10-cm dish. At 24 h after seeding, the cells were transfected with 12.5 nM of siRNA, as described above. At the indicated times after transfection (0, 24, 48, 72, and 96 h), the cells were lysed in an NP-40 lysis buffer (50 mM Tris–HCl, 1% NP-40, 0.25% sodium deoxycholate, 150 mM NaCl, pH 7.4, proteinase inhibitor cocktail; Sigma-Aldrich, MO, USA) and centrifuged at 4°C for 15 min at 15,000×*g*. The protein concentration in the supernatant was determined using a DC protein assay kit (Bio-Rad Laboratories, CA, USA). The protein extract (20 μg) was resuspended in SDS sample buffer and boiled at 95°C for 5 min, and the proteins were then separated by electrophoresis on 7% and 12% SDS-PAGE gels for Ago2 and β-actin, respectively. The proteins were transferred to PDVF Hybond-P membranes (GE Healthcare, CA, USA). Bands were blocked with Tris-buffered saline, pH 7.4, containing 3% nonfat dry milk (Beckton, Dickinson and Company, MD, USA). The membranes were incubated overnight at 4°C with primary antibodies at appropriate concentrations (1:100 for mouse monoclonal anti-Ago2 antibody (Wako, Osaka, Japan) and 1:500 for rabbit polyclonal anti-β-actin antibody (Biolegend, CA, USA)). The membranes were then further incubated with secondary antibodies conjugated with HRP-coupled anti-mouse IgG antibody (1:2,000, ICN Biomedical) or anti-rabbit antibody (1:2,000, Chemicon, CA, USA) at room temperature for 1 h. Finally, the bands were visualized by chemiluminescence using an ECL-Plus System (GE Healthcare).

### RNA isolation, cDNA synthesis, and real-time PCR (quantitative RT-PCR)

RNA isolation and cDNA synthesis were performed according to the manufacturer's instructions. Briefly, cells were seeded at a density of 250,000 cells/dish in a 10-cm dish. At 24 h after the seeding, the cells were transfected with 12.5 nM of siRNA, as described above. At the

indicated times after transfection (0, 24, 48, 72, and 96 h), the total RNA of the HT1080 cells was isolated using an RNeasy Mini Kit with an RNase-Free DNase Set (Qiagen, Hilden, Germany). To conduct the reverse transcription reaction, 0.5 μg of RNA was converted to cDNA in a 1.5-ml microtube with a total volume of 20 μl, including 500 nM of Oligo$(dT)_{20}$, 500 μM dNTP, 1 μl of RNase inhibitor, and 1 μl of ReverTra Ace (Toyobo, Osaka, Japan) for 1 h at 40°C.

Real-time PCR was performed on an ABI 7000 real-time PCR system (Applied Biosystems, CA, USA) with a FastStart TaqMan Probe Master (ROX) and Universal ProbeLibrary (Roche Diagnostics GmbH, Manheim, Germany) according to the manufacturer's instructions. Briefly, the PCR mixture was applied to a 96-well plate in a total volume of 20 μl/well, including a 250 nM probe, 900 nM forward and reverse primers, 2 μl of the generated cDNA, and 10 μl of FastStart TaqMan Probe Master (ROX). The set of primers and a probe for real-time RT-PCR were designed using ProbeFinder software (Roche Diagnostics GmbH). The primers and the probes were as follows: Ago2 primers and probe (forward 5′-GTCTCTGAAGGCCAGTTCCA-3′ and reverse 5′-ATACAGGCCTCACGGATGG-3′, probe #22) and GAPDH primers and probe (forward 5′-GCTCTCTGCTCCTCCTGTTC-3′ and reverse 5′-ACGACCAAATCCGTTGACTC-3′, probe #60). The amplification conditions were as follows: 10 min at 95°C, followed by 40 cycles of 95°C for 15 s and 60°C for 1 min. The quantity was determined from the experimental threshold cycle on a standard curve of the data from a series of serial dilutions of the mixture of generated cDNA. The Ago2 mRNA level was normalized with GAPDH as an endogenous control.

## Cytotoxicity assay (MTT assay)

The cytotoxicity assay was carried out as previously described [34]. Briefly, cells were seeded at a density of 2,500 cells/well in a 96-well plate. At 24 h after seeding, the cells were transfected with various concentrations of siRNA (0, 6.25, 12.5, 25, 50, 100 nM), as described above. At the indicated times after transfection (0, 24, 48, 72, and 96 h), the cells were washed twice with PBS and 50 μl of a stock solution (5 mg/ml in PBS) of 3-(4,5-dimethylthiazol-2-yl 2,5-diphenyl) tetrazolium bromide (MTT, Nacalai Tesque, Kyoto, Japan) was added to each well. After 4 h of incubation at 37°C, the formazan crystals in the medium were dissolved in 150 μl of an acidified isopropanol solution (containing 0.04 N HCl). The formazan production was read in a plate reader using a Wallac 1420 ARVOsx multi-label counter (PerkinElmer, MA, USA) at 590 nm.

## Cell apoptosis analysis

The apoptotic cells were measured using an Annexin V-FITC Apoptosis Detection Kit (Merck, Darmstadt, Germany) according to the manufacturer's instructions. Briefly, cells were seeded at a density of 50,000 cells/well in a six-well plate. At 24 h after seeding, the cells were transfected with 12.5 nM siRNA, as described above. At the indicated times after transfection (24, 48, 72, 96 h), the cells were harvested and treated with Annexin V-FITC solution for 15 min in the dark. Cell fluorescence was detected by a flow cytometer Guava EasyCyte Mini System (Guava Technologies, CA, USA), and the sample data were analyzed using CytoSoft software (Guava Technologies).

## Cell cycle analysis

Cell cycle analysis was performed using a Guava cell cycle reagent kit (Guava Technologies) according to the manufacturer's instructions. Briefly, cells were seeded at a density of 50,000 cells/well in a six-well plate. At 24 h after seeding, the cells were transfected with 12.5 nM siRNA, as described above. At 48 h post-transfection, the cells were harvested, fixed with 70% ethanol, and then treated with Guava cell cycle reagent for 30 min in the dark. Cell cycle analysis for DNA content was measured using a flow cytometer (Guava Technologies). The cell cycle profile (percentage of cells within G0+G1, S, G2+M, and SubG1 phases) was analyzed using CytoSoft software (Guava Technologies).

## Observation of cellular morphology and actin stress fiber by microscopy

The cell specimen for the visualization of actin fiber in cells was prepared as previously described [35]. Briefly, cells were seeded at a density of 5,000 cells/well in a 35-mm glass-based dish (Iwaki, Chiba, Japan) with 200 μl of complete culture medium. At 24 h after seeding, the cells were transfected with 12.5 nM siRNA, as described above. At 48 h post-transfection, the cells were fixed with 4% paraformaldehyde for 30 min at room temperature. Cellular morphology was observed by phase contrast microscopy (LSM510, Carl Zeiss, Oberkochen, Germany). To further visualize the actin stress fiber in the cells, they were permeated with 1% Triton X for 15 min and then stained with 0.2 μM phalloidin-FITC (Sigma-Aldrich) for 1 h at room temperature in a dark room. Actin stress fibers in cells were observed by confocal microscopy (LSM510, Carl Zeiss).

Microarray analysis

A Whole Human Genome Oligo Microarray 44Kx4pack (Agilent Technologies, CA, USA) was used as previously described [36]. Briefly, cells were seeded at a density of 250,000 cells/dish in a 10-cm dish. At 24 h after seeding, the cells were transfected with 12.5 nM of siRNA, as described above. At 48 h post-transfection, the total RNA was isolated using an RNeasy Mini Kit with an RNase-Free DNase Set (Qiagen). The quality of total RNA samples, based on the 28S/18S rRNA ratio, was assessed using an Agilent 2100 Bioanalyzer (Agilent Technologies). The RNAs were amplified, converted to the complementary DNAs, and labeled with Cy3-CTP using a Low RNA Fluorescent Agilent Linear Amplification kit (Agilent Technologies). The amplified complimentary RNA products were labeled with Cy3. The labeled cRNAs were then fragmented and hybridized using Agilent's in situ hybridization plus kit on a Human1A ver.2 Oligo Microarray (Agilent Technologies). The microarrays were scanned with an Agilent Technologies Microarray Scanner (Agilent Technologies) at 5-μm resolution. For comparative analysis between Ago2-siRNA-treated cells and Cont-siRNA-treated cells, the genes that were statistically significant using a two-sample $t$ test ($p<0.05$, $n=3$) were identified and subsequently categorized by gene ontology. The data were analyzed using GeneSpring software (Agilent Technologies).

Antitumor efficacy of intratumor injection of siRNA/cationic liposome complex in a xenograft model

Male Balb/c Slc-nu/nu (20–25 g) mice were purchased from Japan SLC (Shizuoka, Japan). The experimental animals were allowed free access to water and chow and were housed under controlled environmental conditions (constant temperature, humidity, and 12-h dark/light cycle). All animal experiments were evaluated and approved by the Animal and Ethics Review Committee of the University of Tokushima.

To establish the tumor-bearing mouse model, $1\times10^6$ HT1080 cells (in 100 μl DMEM) were subcutaneously inoculated into the right flank of the mice. When the tumor was palpable (about 100 $mm^3$), treatment was started (day 0). For in vivo transfection of siRNA, we used TFL-3 cationic liposome, which has shown high transfection efficiency as the carrier of siRNA, as previously described [27]. TFL-3, consisting of the cationic lipid *O,O'*-ditetradecanoyl-*N*-(α-trimethyl ammonioacetyl) diethanolamine chloride, cholesterol, and dioleoylphosphatidylethanolamine in a molar ratio of 1.00:0.75:0.75 was generously donated by Daiichi-Sankyo Pharmaceutical (Tokyo, Japan) as a lyophilized liposome. Briefly, siRNA solution (40 μg) was directly added to the lyophilized liposomal powder (4 μmol) at a charge ratio of 7.62 (cationic lipid (+)/siRNA (−)) with vigorous vortexing (3,200 rpm, 10 min) to form the siRNA/liposome complex, which is referred to as the lipoplex. The lipoplex including either Ago2-siRNA, Cont-siRNA (40 μg siRNA/mouse/injection), or 9% sucrose solution (50 μl/injection) was directly injected into the xenografts on days 0, 2, 4, 6, 8, and 10. The antitumor effect was evaluated in terms of both tumor volume and survival. Tumor size was assessed in two dimensions and calculated by the following formula: $1/2\times\text{length}\times\text{width}^2$ [37]. Body weight was measured simultaneously and was taken as a parameter of systemic toxicity.

Statistical analysis

All values are expressed as the mean±SD. Statistical analysis was performed via a two-tailed unpaired $t$ test and one-way ANOVA using GraphPad InStat software (GraphPad Software, CA, USA). The level of significance was set at $p<0.05$.

## Results

Gene silencing effect of the transfection of Ago2-siRNA

The Ago2 gene expression in HT1080 cells was initially characterized after the transfection of Ago2-siRNA. Western blotting was performed to examine the Ago2 gene expression at the protein level (Fig. 1a). Expression of Ago2 protein was strongly suppressed in cells at 24 h after the transfection of 12.5 nM of Ago2-siRNA, but was not affected by the transfection of Cont-siRNA. This inhibitory effect of Ago2 protein continued until 96 h post-transfection. The Ago2 gene expression at the mRNA level was also examined after the transfection of Ago2-siRNA (Fig. 1b). qRT-PCR was performed in order to quantify the knock-down efficiency, and consequently, Ago2 mRNA expression was significantly inhibited to 4.4% of Cont-siRNA-treated cells at 24 h after the transfection of Ago2-siRNA. Strong inhibitory effects were observed at 48 h (5.5%) and at 72 h (11.7%) post-transfection, and subsequently, Ago2 mRNA expression was gradually increased to 20.2% even at 96 h post-transfection. Cont-siRNA-treated cells exhibited no significant change in Ago2 mRNA expression compared with untreated cells.

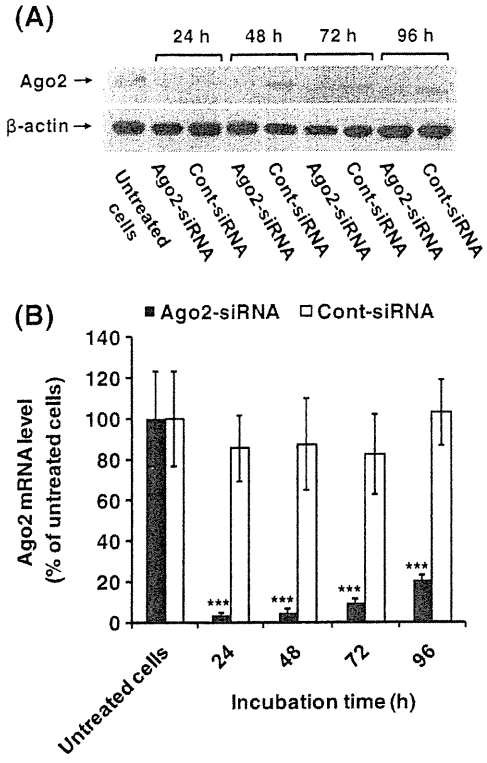


**Fig. 1** Suppression of Ago2 gene expression by the transfection of Ago2-siRNA in HT1080 cells. Expressions of Ago2 protein (100 kDa) and mRNA were detected by Western blot (**a**) and qRT-PCR (**b**) analyses, respectively. Of Ago2-siRNA or Cont-siRNA, 12.5 nM was transfected into cells using Lf2000. At the indicated time post-transfection (24, 48, 72, and 96 h), total protein or RNA in the cells was extracted and analyzed as described in "Materials and methods." Data represent the mean of three separate experiments (Western blot). Each value represents the mean±S.D ($n$=3). ***$p$< 0.005 compared with Cont-siRNA-transfected cells

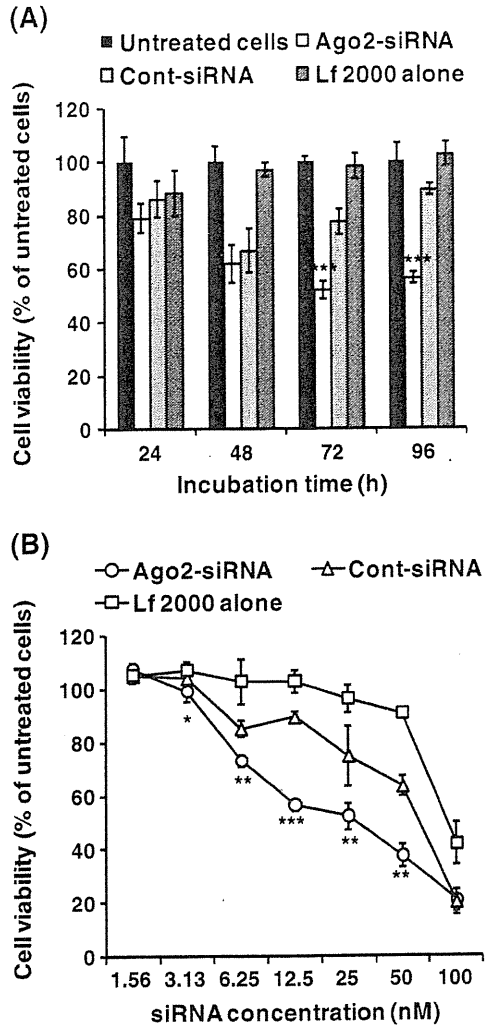


**Fig. 2** Effect of Ago2 gene suppression on cell growth inhibition in HT1080 cells. **a** Time course study of cell viability. Of Ago2-siRNA or Cont-siRNA, 12.5 nM was transfected into cells using Lf2000. At the indicated times post-transfection (24, 48, 72, and 96 h), cell viability was determined by MTT assay as described in the "Materials and methods." **b** Dose dependency of cell viability. Various concentrations of siRNA (0, 6.25, 12.5, 25, 50, and 100 nM) were transfected into cells using Lf2000. At 96 h post-transfection, cell viability was determined by MTT assay as described in "Materials and methods." The amount of Lf2000 in the Lf2000 alone was set as equal to the lipoplex. Each value represents the mean±SD ($n$=3).*$p$<0.05, ***$p$< 0.005 compared with Cont-siRNA-transfected cells

## Inhibition of growth of HT1080 cells by Ago2 gene suppression

The anti-proliferative activity of Ago2 suppression in HT1080 cells was investigated by means of an MTT assay (Fig. 2a). At 24 and 48 h post-transfection, both Ago2-siRNA and Cont-siRNA treatments indicated a similar trend in cell growth inhibition. This might be due to non-specific cytotoxicity derived from the siRNA/Lf2000 transfection reagent complex. It was previously reported that some transfection reagents, including cationic lipid-based liposome, cause cytotoxicity, and the inclusion of nucleic acids such as pDNA further increases cytotoxicity [36, 38]. Such non-selective cytotoxicity induced by transfection might mask the anti-proliferative effect selectively caused by Ago2 gene suppression. In addition, off-target effect induced by transfected siRNA could not be excluded on this non-specific cell growth inhibition. In contrast, at 72 and 96 h post-transfection, while the growth of Cont-siRNA-treated cells had restarted, the growth of Ago2-siRNA-treated cells was still attenuated. The siRNA dose dependency of cell growth was also investigated (Fig. 2b). All treatments inhibited growth in a dose-dependent manner. In particular, Ago2-siRNA treatment showed the most significant inhibitory effect in the range from 6.25 to 50 nM compared with Cont-siRNA. The most significant difference in cell growth between Ago2-siRNA and Cont-siRNA was observed at a dose of 12.5 nM of siRNA ($p$<0.005). The $IC_{50}$ value of each treatment was

24.7 nM for Ago2-siRNA, 59.9 nM for Cont-siRNA, and 93.4 nM for Lf 2000 alone.

## Induction of cell apoptosis by Ago2 gene suppression

The proportion of apoptosis in HT1080 cells induced by Ago2 suppression was also investigated (Fig. 3). At 24 h post-transfection, large numbers of apoptotic cells were observed in both Ago2-siRNA- and Cont-siRNA-treated cells, presumably due to transfection with the siRNA/Lf2000 transfection reagent complex. However, at 48 h after transfection, Ago2-siRNA treatment exhibited a significant apoptotic effect compared with Cont-siRNA. Extensive induction of apoptosis by Ago2 gene suppression was continuously observed up to 96 h.

## Induction of G0/G1 cell cycle arrest by Ago2 gene suppression

The distribution of HT1080 cells in cell cycle stages at 48 h post-transfection was analyzed in order to evaluate intracellular events induced by Ago2 gene suppression (Fig. 4). Ago2-siRNA treatment significantly increased accumulation at the G0/G1 phase (55.2±2.1%) compared with Cont-siRNA treatment (48.0±2.65%). At the same time, the cells at the S and G2/M phases were significantly reduced (S phase, 10.2 ±0.31% by Ago2-siRNA vs. 16.0±3.0% by Cont-siRNA; G2/M phase and 18.8±1.5% by Ago2-siRNA vs. 25.3±1.3% by Cont-siRNA). The cells at the SubG1 phase, which represents apoptotic cells, were significantly increased by Ago2 gene suppression. This finding is consistent with earlier ones (Fig. 3). The difference between Ago2-siRNA treatment and Cont-siRNA treatment at G0/G1 and subG1 was 7.2% and 5.9%, respectively. This indicates that Ago2 gene suppression affects the cell cycle stages of HT1080 cells, resulting in G0/G1 arrest and apoptosis (subG1).

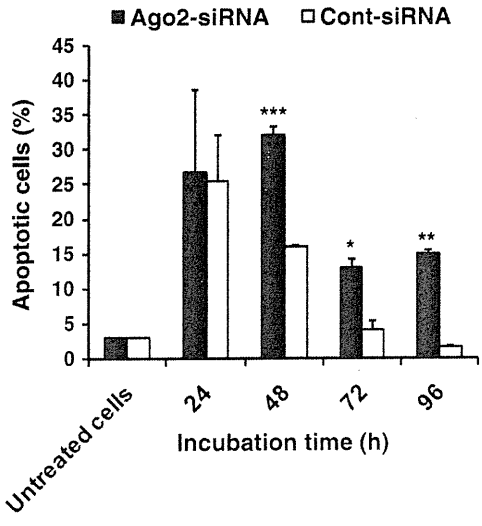


**Fig. 3** Effect of Ago2 gene suppression on the induction of apoptosis in HT1080 cells. Ago2-siRNA or Cont-siRNA (12.5 nM) was transfected into cells using Lf2000. At the indicated times post-transfection (24, 48, 72, and 96 h), the proportion of apoptotic cells that were mean Annexin V-FITC positive cells was measured by flow cytometry as described in "Materials and methods." Each value represents the mean±SD ($n$=3).*$p$<0.05, ***$p$<0.005 compared with Cont-siRNA-transfected cells

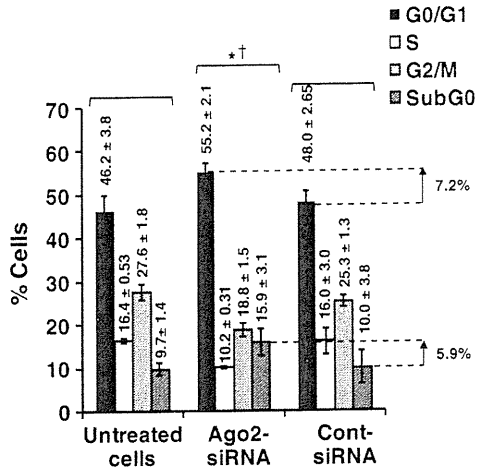


**Fig. 4** Effect of Ago2 gene suppression on the distribution of cells in cell cycle stages in HT1080 cells. Ago2-siRNA or Cont-siRNA (12.5 nM) was transfected into cells using Lf2000. At 48 h post-transfection, the distribution of cell cycle stages in the cells was analyzed by flow cytometry as described in the "Materials and methods." Each value represents the mean±SD ($n$=3).*$p$<0.05 compared with Cont-siRNA transfected cells. †$p$<0.05 compared with untreated cells

## Morphological change in cells by Ago2 gene suppression

The morphology of HT1080 cells after Ago2 gene knockdown was observed. Ago2-siRNA-treated cells were flattened and assembled together and were distinguishable in appearance from untreated cells or Cont-siRNA-treated cells (Fig. 5a–c). To confirm the remarkable stress on cells treated with Ago2-siRNA, the actin cytoskeleton was stained. The formation of actin stress fibers was observed in Ago2-siRNA-treated cells, but not in the Cont-siRNA-treated cells or untreated cells (Fig. 5d–f). This finding indicates that Ago2 gene suppression induces strong cellular stress.

## Change of the gene expression profile on cells treated with Ago2-siRNA

cDNA microarray analysis was carried out in order to investigate the change in global gene expression induced by Ago2 gene suppression. Approximately 25,000 genes were validated within the range of detection limits following Ago2-siRNA treatment and Cont-siRNA treatment. The cells treated with Ago2-siRNA (Fig. 6a) showed a remarkable gene

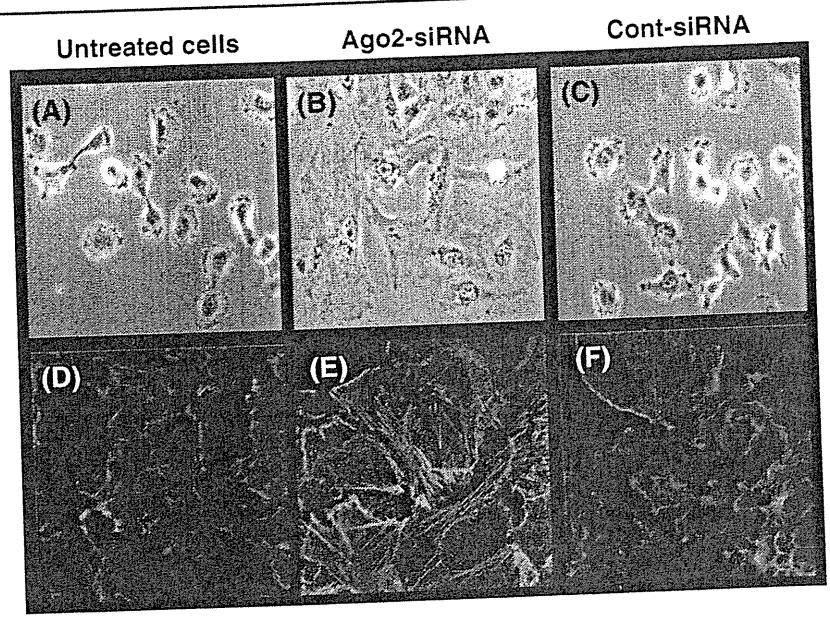


**Fig. 5** Effect of Ago2 gene suppression on the cellular morphology in HT1080 cells. Ago2-siRNA or Cont-siRNA (12.5 nM) was transfected into cells using Lf2000. At 48 h post-transfection, cellular morphology was observed by phase contrast microscopy (×630 magnification, *upper panels*) (**a**–**c**). Actin organization was also visualized by staining with phalloidin-FITC, as described in "Materials and methods," and then fluorescence was observed by confocal microscopy (×630 magnification, *lower panels*) (**d**–**f**)

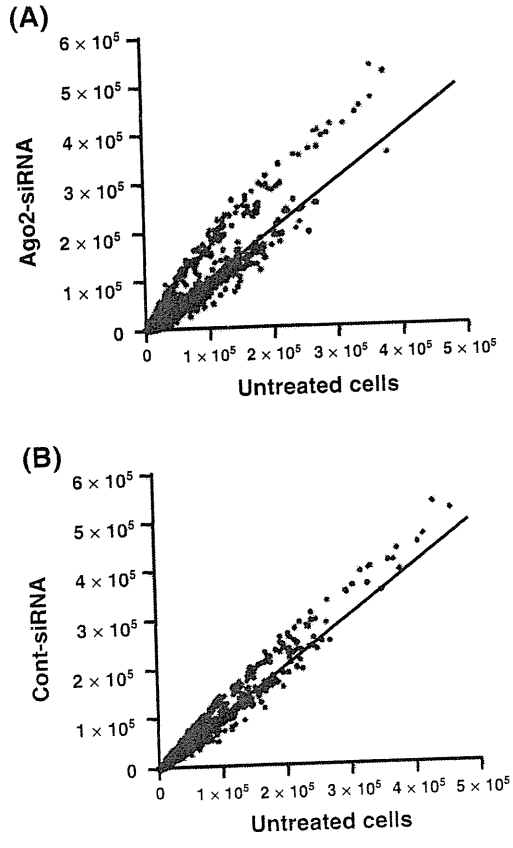


**Fig. 6** Raw data scatter plot of array signals of HT1080 cells treated with Ago2-siRNA. A large number of genes (25,655) are shown. Ago2-siRNA or Cont-siRNA (12.5 nM) was transfected into cells using Lf2000. At 48 h post-transfection, total RNA was extracted and then analyzed by microarray as described in "Materials and methods." The *lines* drawn in the figure indicate the intensity ratios of genes exhibiting no changes

alteration pattern compared with the cells treated with Cont-siRNA (Fig. 6b). Filtration analysis further indicated that Ago2-siRNA treatment induced remarkable alterations in global gene expression (Table 1). The genes that were significantly up-regulated or down-regulated ($p<0.05$) in Ago2-siRNA-treated cells, as compared with those in Cont-siRNA-treated cells, were identified and categorized on the basis of gene ontology (Table 2). The genes were mostly related to apoptosis, the cell cycle, immune response, angiogenesis, cell adhesion, and metabolism.

## In vivo antitumor effect of Ago2 siRNA in HT1080 xenograft model

To evaluate the in vivo therapeutic effect of Ago2 suppression, Ago2-siRNA (or Cont-siRNA)/TFL-3 cationic liposome complex (lipoplex) was injected into HT1080 tumors, which grew up under the skin. As shown in Fig. 7a,

**Table 1** Up-regulated and down-regulated genes by distinct filtrations in HT1080 cells treated with Ago2-siRNA, Cont-siRNA, and Lf2000 alone

| | Ago2-siRNA | Cont-siRNA |
|---|---|---|
| Changed >1.5-fold | 3,007 | 1,354 |
| Changed <1/1.5-fold | 3,209 | 1,268 |
| Total (%) | 6,216 (24.23) | 2,622 (10.22) |
| Changed >2-fold | 998 | 228 |
| Changed <1/2-fold | 967 | 294 |
| Total (%) | 1,965 (7.66) | 522 (2.03) |

The total number of genes validated is 25,655

**Table 2** Global change of all genes treated with Ago2-siRNA ($p<0.05$) or Cont-siRNA vs. untreated cells

| GenBank | Symbol | Gene name | Fold change | | | $p$ value[b] |
|---|---|---|---|---|---|---|
| | | | Ago2-siRNA[a] | Cont-siRNA[a] | (Ago2/Cont) | |
| Apoptosis | | | | | | |
| NM_001003940 | *BMF* | Bcl2 modifying factor isoform bmf-1 | 16.36 | 3.34 | 4.90 | 0.03 |
| NM_000043 | *FAS* | Tumor necrosis factor receptor superfamily Member 6 isoform 1 precursor | 2.19 | 1.58 | 1.39 | 1.11E−03 |
| NM_001429 | *EP300* | E1A binding protein p300 | 1.51 | 0.99 | 1.53 | 1.82E−04 |
| Cell cycle | | | | | | |
| NM_000389 | *CDKN1A* | Cyclin-dependent kinase inhibitor 1A | 2.66 | 1.42 | 1.87 | 4.24E−07 |
| AF011794 | *CCPG1* | Cell cycle progression restoration 8 protein | 2.06 | 1.62 | 1.27 | 0.01 |
| NM_004064 | *CDKN1B* | Cyclin-dependent kinase inhibitor 1B | 2.02 | 1.00 | 2.02 | 2.18E−07 |
| NM_005225 | *E2F1* | E2F transcription factor 1 | 0.41 | 0.60 | 0.68 | 0.02 |
| Immune response | | | | | | |
| NM_005532 | *IFI27* | Interferon, alpha-inducible protein 27 | 3.15 | 1.75 | 1.80 | 1.09E−06 |
| NM_002982 | *CCL2* | Small inducible cytokine A2 precursor | 1.70 | 1.27 | 1.34 | 3.84E−03 |
| NM_002502 | *NFKB2* | Nuclear factor of kappa light polypeptide Gene enhancer in B cells 2 (p49/p100) | 1.55 | 1.02 | 1.52 | 1.01E−04 |
| NM_213662 | *STAT3* | Signal transducer and activator of Transcription 3 isoform 3 | 1.43 | 1.05 | 1.37 | 1.99E−03 |
| NM_139266 | *STAT1* | Signal transducer and activator of Transcription 1 isoform beta | 1.35 | 1.08 | 1.25 | 0.02 |
| Angiogenesis | | | | | | |
| NM_000029 | *AGT* | Angiotensinogen preproprotein | 8.10 | 3.82 | 2.12 | 4.06E−08 |
| NM_003246 | *THBS1* | Thrombospondin 1 precursor | 2.88 | 0.66 | 4.39 | 4.23E−14 |
| NM_001955 | *EDN1* | Endothelin 1 | 2.23 | 1.03 | 2.17 | 1.45E−08 |
| Cell adhesion | | | | | | |
| NM_212482 | *FN1* | Fibronectin 1 isoform 1 preproprotein | 2.84 | 1.82 | 1.56 | 4.33E−05 |
| NM_002210 | *ITGAV* | Integrin alpha-V precursor | 2.75 | 1.04 | 2.65 | 2.75E−10 |
| NM_000212 | *ITGB3* | Integrin beta chain, beta 3 precursor | 2.38 | 1.60 | 1.48 | 2.19E−04 |
| NM_004530 | *MMP2* | Matrix metalloproteinase 2 preproprotein | 2.20 | 1.06 | 2.08 | 4.11E−08 |
| Z74615 | *COL1A1* | Prepro-alpha1(I) collagen | 2.16 | 1.01 | 2.15 | 8.14E−08 |
| NM_133376 | *ITGB1* | Integrin beta 1 isoform 1A precursor | 1.42 | 1.18 | 1.20 | 0.049 |
| Metabolism | | | | | | |
| NM_002317 | *LOX* | Lysyl oxidase preproprotein | 1.91 | 1.11 | 1.72 | 3.43E−06 |
| NM_146421 | *GSTM1* | Glutathione S-transferase M1 isoform 2 | 1.76 | 1.36 | 1.29 | 9.30E−03 |
| NM_002318 | *LOXL2* | Lysyl oxidase-like 2 precursor | 1.48 | 1.15 | 1.29 | 8.22E−03 |
| NM_000311 | *PRNP* | Prion protein preproprotein | 0.14 | 0.99 | 0.14 | 1.01E−03 |
| Others | | | | | | |
| NM_000602 | *SERPINE1* | Plasminogen activator inhibitor-1 | 3.13 | 2.01 | 1.56 | 4.51E−05 |
| NM_002116 | *HLA-A* | Major histocompatibility complex, class I, A precursor | 1.55 | 1.28 | 1.21 | 0.04 |
| NM_000021 | *PSEN1* | Presenilin 1 | 1.43 | 1.09 | 1.31 | 6.03E−03 |

[a] Fold change compared with untreated cells

[b] Significant difference between the cells treated with Ago2-siRNA vs. Cont-siRNA

Ago2-siRNA treatment showed a remarkable tumor growth inhibition. In addition, Ago2-siRNA treatment increased the survival time of tumor-bearing mice (median survival time, 38.7 days for Cont-siRNA treatment and 28.6 days for sucrose), and as a result, more than 50% of mice (four out of seven) became long-term survivors (>70 days). Remarkable body weight loss was not observed with any treatment (data not shown).

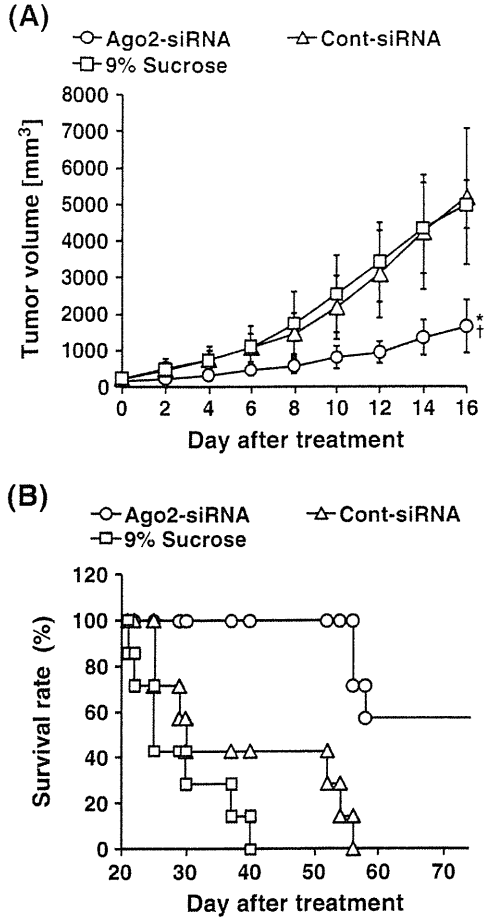


**Fig. 7** Antitumor effect of Ago2-siRNA lipoplex in HT1080 xenograft model. On days 0, 2, 4, 6, 8, and 10, either Ago2-siRNA or Cont-siRNA lipoplex (40 μg siRNA per mouse per injection) or 9% sucrose solution was directly injected into the xenograft. Each treatment group included seven mice. Antitumor activity was assessed by determining the tumor size (**a**) and survival of the mice (**b**). Each value represents the mean±SD ($n$=7). *$p$<0.05 compared with treatment with Cont-siRNA lipoplex. †$p$<0.05 compared with treatment with 9% sucrose

## Discussion

The present study showed that the suppression of the Ago2 gene significantly reduced the growth of human fibrosarcoma cells (HT1080) in vitro and in vivo, as shown in Figs. 2 and 7. This suggests that Ago2 is a desirable target for siRNA-based cancer therapy. In considering clinical application, attention should of course be paid to the influence of Ago2 gene suppression in normal tissue, which may lead to severe tissue damage. There have been very few reports that demonstrate phenotype changes after Ago2 knockout. Liu et al. [23] observed that Ago2-null mice are embryonic lethal. O'Carroll et al. [26] demonstrated that bone marrow conditional Ago2$^{-/-}$ mice have defective B cell differentiation. The duration of gene knockdown induced by siRNA is relatively shorter and more temporal than gene knockout generated genetically. The risk of damage caused by Ago2 gene suppression may be mitigated by this shorter duration in siRNA-mediated gene suppression. Such risk might also be relieved by the combination of Ago2-siRNA with a delivery system that could selectively deliver siRNA to a targeted tissue [4].

Ago2 gene suppression affected the shape of HT1080 cells. Ago2-siRNA-treated cells were flattened and thinned and gained cell–cell adhesion (Fig. 5a). The microarray study indicated enhanced expression of the genes including cell–cell adhesion in the cells (Table 2). Adam et al. [39] recently demonstrated in a breast cancer cell line that Ago2 overexpression showed a transformed phenotype, and the cells lost cell–cell adhesion as a result of down-regulation of the gene relating to cell–cell adhesion. These findings suggest that the Ago2 gene is strongly related to cell–cell adhesion in tumor cells. The loss of cell–cell adhesion and enhanced motility are known as the hallmarks of the tumorigenic progression of epithelial and endothelial cells [40]. The tumorigenic property of HT1080 cells might be relieved by treatment with siRNA against Ago2. This may result in efficient tumor growth suppression in an HT1080 xenograft model (Fig. 7). Cellular phenotypic changes induced by Ago2 gene suppression were characterized in vitro. Ago2 gene suppression exhibited an anti-proliferation effect (Fig. 2) as a result of the induction of apoptosis (Fig. 3) and G0/G1 cell cycle arrest (Fig. 4). Microarray analysis indicated a possibility that the activation of apoptosis-related genes such as Bmf and FAS is involved in the induction of apoptosis by Ago2 gene suppression (Fig. 3). Bmf (the BH3-only protein) is categorized as a pro-apoptotic member of the Bcl-2 family [41] which is involved in mitochondria-mediated apoptosis. The BH3-only protein also served as a sensor for various apoptotic stimuli, and the activation of this gene resulted in cytoskeleton damage [42]. The formation of actin stress fibers observed in Fig. 5e might result from the activation of the Bmf gene. The FAS gene is known to induce a death receptor apoptotic pathway, which is another major caspase-mediated apoptotic pathway [43]. The detection of genes involved in multiple apoptotic pathways may indicate that Ago2 gene suppression provides complex stimuli to cells. Unfortunately, overexpression of the genes that regulate the downstream apoptosis signaling pathway could not be detected under the present experimental conditions (at 48 h post-transfection). This might be due to time discrimination in the progression of the apoptosis signaling pathway. The microarray study also identified some cell cycle-related genes, CDKN1A, CCPG1, and E2F1 (Table 2). The set of CDKN1A (p21) and CDKN1B (p27) are widely known as the G1 checkpoint CDK inhibitors that regulate G1 arrest [44, 45]. E2F1 is known

as the transcriptional factor that keeps the cells in the G1 phase incorporated with Rb proteins [46]. Mack et al. [47] reported that the cell cycle of fibrosarcoma is strictly regulated by these cell cycle-related genes (CDKN1A, CCPG1, and E2F1). In addition, Abukhdeir and Park [48] reported that G0/G1 cell arrest by CDKN1A (p21) and CDKN1B (p27) is one of the major causes of the induction of cellular apoptosis in some types of cells. Therefore, following Ago2 gene suppression, HT1080 cells, halted at the G0/G1 phase, might induce apoptosis (Figs. 3 and 4). It is of interest that the *PRNP* gene was most inhibited by Ago2 gene suppression (0.14-fold, Table 2). The *PRNP* gene was originally categorized in metabolism, which is related to oxidative stress. In addition, the importance of the *PRNP* gene in cancer growth is being increasingly recognized. Studies have reported that the *PRNP* gene was overexpressed in colorectal cancer [49] and gastric cancer [50]. The overexpression of this gene accelerated cell proliferation by promoting the G1/S phase transition via the regulation of cyclin D1 [50]. These findings indicate that the down-regulation of *PRNP* by Ago2 gene suppression might attenuate the cell cycle and cell proliferation. These would be possible pathways accounting for the anti-proliferation effect mediated by Ago2 gene suppression (Fig. 2).

It is known that Ago2 broadly regulates multiple miRNAs and miRNA-mediated pathways, including cell survival and cancer progression. miRNAs, which are incorporated with Ago2, down-regulate various mRNAs [19]. Suppression of the Ago2 protein would thus lead to the accumulation of a large amount of uncleaved mRNA inside the cells and result in the breakdown of cellular function. This microarray study demonstrated that Ago2 gene suppression enhanced the global gene expressions of more than 990 genes (>2-fold changes; Fig. 6 and Table 1). The present study could not exclude the possibility that non-specific increases in the entire gene expression induce changes in cellular morphology, resulting in cellular death.

## Conclusion

We found that Ago2 gene suppression mediated by Ago2-siRNA inhibited the growth of human fibrosarcoma cells in vitro and in vivo. This biological outcome was likely associated with phenotypical changes, including apoptosis, G0/G1 cell cycle accumulation, and morphological changes. The Ago2 gene, therefore, may be a desirable potential therapeutic target for siRNA-based cancer therapy.

**Acknowledgments** The authors thank Dr. James L. McDonald for his helpful advice in improving the manuscript. This research was supported by Research on Advanced Medical Technology in Health and Labor Science Research Grants, Ministry of Health, Labor and Welfare, Japan.

**Conflict of interest** Authors declare no conflict.

## References

1. Taconis WK, van Rijssel TG. Fibrosarcoma of long bones. A study of the significance of areas of malignant fibrous histiocytoma. J Bone Joint Surg Br. 1985;67(1):111–6.
2. Mocellin S, Rossi CR, Brandes A, Nitti D. Adult soft tissue sarcomas: conventional therapies and molecularly targeted approaches. Cancer Treat Rev. 2006;32(1):9–27.
3. Meister G, Tuschl T. Mechanisms of gene silencing by double-stranded RNA. Nature. 2004;431(7006):343–9.
4. Akhtar S, Benter IF. Nonviral delivery of synthetic siRNAs in vivo. J Clin Invest. 2007;117(12):3623–32.
5. Huang C, Li M, Chen C, Yao Q. Small interfering RNA therapy in cancer: mechanism, potential targets, and clinical applications. Expert Opin Ther Targets. 2008;12(5):637–45.
6. Saxena N, Lahiri SS, Hambarde S, Tripathi RP. RAS: target for cancer therapy. Cancer Investig. 2008;26(9):948–55.
7. Pelengaris S, Khan M. The c-MYC oncoprotein as a treatment target in cancer and other disorders of cell growth. Expert Opin Ther Targets. 2003;7(5):623–42.
8. Aigner A. Applications of RNA interference: current state and prospects for siRNA-based strategies in vivo. Appl Microbiol Biotechnol. 2007;76(1):9–21.
9. Takei Y, Kadomatsu K, Yuzawa Y, Matsuo S, Muramatsu T. A small interfering RNA targeting vascular endothelial growth factor as cancer therapeutics. Cancer Res. 2004;64(10):3365–70.
10. Mendelsohn J, Baselga J. Epidermal growth factor receptor targeting in cancer. Semin Oncol. 2006;33(4):369–85.
11. Kargiotis O, Chetty C, Gondi CS, Tsung AJ, Dinh DH, Gujrati M, et al. Adenovirus-mediated transfer of siRNA against MMP-2 mRNA results in impaired invasion and tumor-induced angiogenesis, induces apoptosis in vitro and inhibits tumor growth in vivo in glioblastoma. Oncogene. 2008;27(35):4830–40.
12. Ryan BM, O'Donovan N, Duffy MJ. Survivin: a new target for anti-cancer therapy. Cancer Treat Rev. 2009;35(7):553–62.
13. Sonoke S, Ueda T, Fujiwara K, Sato Y, Takagaki K, Hirabayashi K, et al. Tumor regression in mice by delivery of Bcl-2 small interfering RNA with pegylated cationic liposomes. Cancer Res. 2008;68(21):8843–51.
14. Zhang Y, Wang Y, Gao W, Zhang R, Han X, Jia M, et al. Transfer of siRNA against XIAP induces apoptosis and reduces tumor cells growth potential in human breast cancer in vitro and in vivo. Breast Cancer Res Treat. 2006;96(3):267–77.
15. Stege A, Priebsch A, Nieth C, Lage H. Stable and complete overcoming of MDR1/P-glycoprotein-mediated multidrug resistance in human gastric carcinoma cells by RNA interference. Cancer Gene Ther. 2004;11(11):699–706.
16. Degenhardt Y, Lampkin T. Targeting Polo-like kinase in cancer therapy. Clin Cancer Res. 2010;16(2):384–9.
17. Scholl C, Frohling S, Dunn IF, Schinzel AC, Barbie DA, Kim SY, et al. Synthetic lethal interaction between oncogenic KRAS dependency and STK33 suppression in human cancer cells. Cell. 2009;137(5):821–34.
18. Tokatlian T, Segura T. siRNA applications in nanomedicine. Wiley Interdiscip Rev Nanomed Nanobiotechnol. 2010;2(3):305–15.
19. Sevignani C, Calin GA, Siracusa LD, Croce CM. Mammalian microRNAs: a small world for fine-tuning gene expression. Mamm Genome. 2006;17(3):189–202.
20. Bartel DP. MicroRNAs: genomics, biogenesis, mechanism, and function. Cell. 2004;116(2):281–97.